SIAM J. NUMER. ANAL.
Vol. 57, No. 3, pp. 1289–1317

ON THE VARIABLE TWO-STEP IMEX BDF METHOD FOR PARABOLIC INTEGRO-DIFFERENTIAL EQUATIONS WITH NONSMOOTH INITIAL DATA ARISING IN FINANCE*

WANSHENG WANG†, YINGZI CHEN‡, AND HUA FANG§

Abstract. In this paper the implicit-explicit (IMEX) two-step backward differentiation formula (BDF2) method with variable step-size, due to the nonsmoothness of the initial data, is developed for solving parabolic partial integro-differential equations (PIDEs), which describe the jump-diffusion option pricing model in finance. It is shown that the variable step-size IMEX BDF2 method is stable for abstract PIDEs under suitable time step restrictions. Based on the time regularity analysis of abstract PIDEs, the consistency error and the global error bounds for the variable step-size IMEX BDF2 method are provided. After time semidiscretization, spatial differential operators are treated by using finite difference methods, and the jump integral is computed using the composite trapezoidal rule. A local mesh refinement strategy is also considered near the strike price because of the nonsmoothness of the payoff function. Numerical results illustrate the effectiveness of the proposed method for European and American options under jump-diffusion models.

Key words. partial integro-differential equation, implicit-explicit methods, two-step backward differentiation formula, options pricing, jump-diffusion model, error estimates, parabolic equations, finite difference method, stability

AMS subject classifications. 65M06, 65M55, 65L60, 91B25, 91G60, 65J10

DOI. 10.1137/18M1194328

1. Introduction.

In this paper, we consider the numerical solution of parabolic integro-differential equations (PIDEs) containing a nonlocal integral operator, which arise in asset pricing problems in mathematical finance. The discretization of such nonlocal integral operators with standard finite difference schemes, which is the most common way to discretize the differential operators in the option pricing context (see, for example, [45, 1]), entails densely populated systems which unduly increase the computational complexity of an implicit time stepping scheme. Some methods have already been designed to solve the resulting systems with full matrices, such as alternating direct implicit (ADI) method [3], FFT, [14, 2], iterative methods [45, 13, 2, 46, 40], and multigrid methods [47, 9].

To avoid the inversion of a full matrix, the implicit-explicit (IMEX) time discretizations that typically treat the nonlocal integral operator explicitly and the rest of the operators implicitly are exploited as an increasingly popular alternative. Since the resulting tridiagonal systems can be solved directly and extremely efficiently, research on the IMEX scheme has become very active. A first-order IMEX time

*Received by the editors June 14, 2018; accepted for publication (in revised form) March 21, 2019; published electronically June 6, 2019.

http://www.siam.org/journals/sinum/57-3/M119432.html

Funding: This work was supported by National Natural Science Foundation of China, grants 11771060 and 11371074.

†Department of Mathematics, Shanghai Normal University, Shanghai 200234, China, and School of Mathematics and Statistics, Changsha University of Science & Technology, 410076 Hunan, China (w.s.wang@163.com).

‡School of Mathematics and Computational Science, Hunan Key Laboratory for Computation and Simulation in Science and Engineering, Xiangtan University, 411105 Hunan, China (1020821222@qq.com).

§School of Mathematics and Statistics, Changsha University of Science & Technology, 410076 Hunan, China (1037560603@qq.com).

discretization method that treats the integral term explicitly and the differential terms implicitly for American options with Merton's model is proposed in [50]. Cont and Voltchkova [12] proposed an IMEX time integral method for pricing European options in exponential Lévy models. IMEX Runge–Kutta methods were used to solve PIDEs by Briani, Natalini, and Russo in [7]. To increase accuracy, Feng and Linetsky considered combining the first-order IMEX Euler scheme with the Richardson extrapolation method for solving PIDEs in [17] (see, also, [45, 31]). An IMEX time stepping scheme, together with a fitted finite volume method for the spatial discretization for solving PIDEs, was investigated in [49]. Salmi and Toivanen [41] proposed families of IMEX time discretization schemes defined by a convex combination parameter, which divides the zeroth-order term due to the jumps between the implicit and explicit parts, for PIDEs and obtained several interesting results. Salmi, Toivanen, and Sydow [42] used a two-step IMEX Crank–Nicolson–Adams–Bashforth (CNAB) method to solve PIDEs under stochastic volatility models with jumps. Pindza, Patidar, and Ngounda [37] proposed a spectral collocation method in space in combination with the IMEX predictor-corrector time-marching method for pricing European vanilla and butterfly spread options under Merton's jump-diffusion model. Kadalbajoo, Tripathi, and Kumar [23] proposed and analyzed three IMEX time semidiscretizations for solving PIDEs under Merton's and Kou's jump-diffusion models. IMEX CNAB numerical pricing of European and American options under the Bates model was investigated in [44]. Kadalbajoo, Kumar, and Tripathi [25] presented a radial basis function based IMEX two-step backward differentiation formula (BDF2) to solve PIDEs under jump-diffusion models. A splitting implicit-explicit (SIMEX) scheme for solving a partial integro-differential Fokker–Planck equation related to a jump-diffusion process was investigated in [19]. Combining IMEX time stepping methods with meshless space discretization techniques for solving PIDEs was recently studied in [38, 39].

These IMEX schemes analyzed in the literature are based on the uniform time grids. However, due to the nonsmoothness of the initial data, that is, the payoff function in option models, singularities may arise at $\tau = 0$, and variable time grids are needed. In fact, variable step-sizes are often essential to obtain computationally efficient, accurate results for solutions of time-dependent differential equations with different time scales, i.e., solutions rapidly varying in some regions of time while slowly changing in other regions. The time analyticity of the solution to PIDEs arising in finance has been exploited by Matache, Schwab, and Wihler in [34], and the so-called geometric time grids are used to resolve the low regularity of the solution at $\tau = 0$. In their work, the *hp*-discontinuous Galerkin time stepping scheme is exploited. A similar deliberate time grid was also considered in [46]. In this paper we study a variable step-size IMEX two-step backward differentiation formula (BDF2) for solving PIDEs. To the best of our knowledge, this is the first paper on a variable step-size IMEX scheme for evaluating financial derivatives. We show the stability of the variable step-size IMEX BDF2 method for abstract PIDEs and derive the L^2 error bounds for this method for nonsmooth initial data. This work can be seen as an extension of the paper [23], which showed that the IMEX BDF2 is stable and second-order accurate for solving PIDEs with constant step-sizes and at few initial time steps with IMEX Euler scheme on a finer grid due to the nonsmoothness of the initial data. As pointed out in this paper, for almost all financial model problems, the given data are nonsmooth, and singularities may arise at $\tau = 0$. Consequently, such an extension is particularly important since the error bounds on the variable step-size IMEX BDF2 method for PIDEs with nonsmooth initial data will be more practical, robust, and sharp.

The remainder of this paper is organized as follows. Section 2 introduces mathematical models for option pricing problems under a jump-diffusion process. An abstract PIDE which describes the jump-diffusion models is further introduced, and some assumptions are made on the differential operators, the integral operator, and the initial data in section 3. The time regularity of the solution is also analyzed in this section. In section 4, we propose the variable step-size IMEX BDF2 method for solving PIDEs and study its stability and error bounds. Two types of time variable grid are considered in section 5. Section 6 is devoted to a fully discrete scheme based on the finite difference method for space discretization. A numerical study is carried out for several test cases in section 7. Section 8 contains a few concluding remarks.

2. The continuous mathematical model for option pricing problems. The amount of financial option trading has grown to an enormous scale since the pioneering work by Black and Scholes [6] and Merton [35] on the pricing of options in 1973. The celebrated Black–Scholes model is based on the assumption that the price of the underlying asset behaves like a geometric Brownian motion with a drift and a constant volatility which cannot explain the market prices of options with various strike prices and maturities. To explain these behaviors, a number of alternative models have been introduced in the financial literature, for example, nonlinear models [32, 33, 4, 18] and jump-diffusion models [36, 27, 11], which are given by a PIDE. However, these models are more difficult to handle numerically in contrast to the celebrated Black–Scholes model. We have proposed two classes of splitting methods for solving nonlinear option pricing problems [20, 21]. In this paper, we consider an IMEX scheme for solving jump-diffusion models and provide an efficient method for numerically solving PIDEs.

Let $U(t,S)$ be the value of a European contract that depends on the time t and underlying asset price S, which is given by a process of the form

$$\frac{dS}{S} = \nu dt + \sigma dz + (\eta - 1)dq, \tag{2.1}$$

where ν is the drift rate, σ is the volatility of the Brownian part of the process, $\eta - 1$ is an impulse function giving a jump from S to $S\eta$, and q is a Poisson process and assumed to be independent of the Wiener process z. Here, $dq = 0$ with probability $1 - \lambda dt$, and $dq = 1$ with probability λdt, where λ is the Poisson arrival intensity. Under the above assumptions it is well known [36] that $U(t,S)$ satisfies a final value problem defined by the following PIDE:

$$\frac{\partial U}{\partial t} + \frac{1}{2}\sigma^2 S^2 \frac{\partial^2 U}{\partial S^2} + (r_I - \lambda\kappa)S\frac{\partial U}{\partial S} - (r_I + \lambda)U + \lambda J(U(t,S)) = 0, \tag{2.2}$$

where r_I is the risk-free interest rate, κ denotes the average relative jump size, $\mathbb{E}(\eta - 1)$, and $J(U(t,S))$ denotes the integral

$$J(U(t,S)) = \int_0^\infty U(t,S\eta)p(\eta)d\eta.$$

Here $p(\eta)$ is the probability density function of the jump amplitude η; thus for all η, $p(\eta) \geq 0$, and $\int_0^\infty p(\eta)d\eta = 1$. In the model originally presented by Merton [36] the probability density function of the jump is

$$p(\eta) = \frac{1}{\sqrt{2\pi}\sigma_{\mathrm{Me}}\eta} e^{-[\ln\eta - \mu_{\mathrm{Me}}]^2/2\sigma_{\mathrm{Me}}^2}. \tag{2.3}$$

The expected relative change in the stock price is $\kappa = \mathbb{E}(\eta - 1) = e^{\mu_{\text{Me}} + \sigma_{\text{Me}}^2/2} - 1$, where μ_{Me} and σ_{Me}^2 are the mean and the variance of jump in return. Under a modified version of Kou's jump-diffusion model, $p(\eta)$ is the following log-double-exponential density:

$$p(\eta) := \frac{1}{\eta}\left(a\eta_1 e^{-\eta_1 \ln \eta}\mathcal{H}(\ln \eta) + b\eta_1 e^{\eta_2 \ln \eta}\mathcal{H}(-\ln \eta)\right), \tag{2.4}$$

where $\eta_1 > 1$, $\eta_2 > 0$, $a > 0$, $b = 1 - a$, and $\mathcal{H}(\cdot)$ is the Heaviside function. In this case, it can be shown that $\kappa = \frac{a\eta_1}{\eta_1 - 1} + \frac{b\eta_2}{\eta_1 + 1} - 1$.

The value U at the expiry date is given by

$$U(T, S) = \phi(S), \quad S \in [0, \infty),$$

where $\phi(S)$ is the payoff function for the option contract. In the case of European option, the payoff function is

$$U(T, S) = \begin{cases} (S - K)^+ & \text{in the case of a call option,} \\ (K - S)^+ & \text{in the case of a put option.} \end{cases} \tag{2.5}$$

The payoff function of (2.5) has a slop discontinuity at $S = K$.

By making the changes of variables $x = \ln(S/K)$, $y = \ln \eta$ $(0 < \eta < \infty)$, $\tau = T - t$, $U(T - t, Ke^x) = u(\tau, x)$, evaluation of the option values requires solving the PIDE

$$\frac{\partial u}{\partial \tau} - \frac{1}{2}\sigma^2 \frac{\partial^2 u}{\partial x^2} - \left(r_I - \frac{1}{2}\sigma^2 - \lambda\kappa\right)\frac{\partial u}{\partial x} + (r_I + \lambda)u - \lambda \int_{-\infty}^{+\infty} u(\tau, x + y) f(y) dy = 0, \tag{2.6}$$

where $f(y) = e^y p(e^y)$. Now the terminal condition (2.5) becomes the initial condition

$$u(0, x) = g(x) = \phi(e^x) = \begin{cases} (Ke^x - K)^+ & \text{in the case of a call option,} \\ (K - Ke^x)^+ & \text{in the case of a put option.} \end{cases} \tag{2.7}$$

The boundary conditions for the call option are given by

$$u(\tau, x) \to 0 \text{ as } x \to -\infty \quad \text{and} \quad u(\tau, x) \to Ke^x - Ke^{-r_I \tau} \text{ as } x \to +\infty, \tag{2.8}$$

and for the put option by

$$u(\tau, x) \to Ke^{-r_I \tau} - Ke^x \text{ as } x \to -\infty \quad \text{and} \quad u(\tau, x) \to 0 \text{ as } x \to +\infty. \tag{2.9}$$

To construct a numerical scheme for approximation of the PIDE (2.6), we first truncate the infinite domain $\mathbb{R}$ for x to be $\Omega := (X_l, X_r)$ with a sufficiently small X_l and a sufficiently large X_r. On the truncated domain Ω, we solve the PIDE

$$\frac{\partial u(\tau, x)}{\partial \tau} + \mathcal{L}u(\tau, x) - \lambda \mathcal{I}u(\tau, x) = \lambda R(\tau, x), \quad (\tau, x) \in [0, T) \times \Omega, \tag{2.10}$$

$$u(0, x) = g(x), \qquad x \in \bar{\Omega} := [X_l, X_r], \tag{2.11}$$

where the differential operator $\mathcal{L}$ and the integral operator $\mathcal{I}$ are, respectively, defined by

$$\mathcal{L}u(\tau, x) = -\frac{1}{2}\sigma^2 \frac{\partial^2 u}{\partial x^2} - \left(r_I - \frac{1}{2}\sigma^2 - \lambda\kappa\right)\frac{\partial u}{\partial x} + (r_I + \lambda)u, \tag{2.12}$$

$$\mathcal{I}u(\tau, x) = \int_{\Omega} u(\tau, x + y) f(y) dy. \tag{2.13}$$

Here, by taking into account the asymptotic behavior of the option, the remainder $R(\tau, x)$ is given by

$$R(\tau,x)=\int_{-\infty}^{+\infty}u(\tau,x+y)f(y)dy-\mathcal{I}u(\tau,x). \tag{2.14}$$

For Merton's model and Kou's model, $R(\tau, x)$ can be computed directly. For European call option, they can be expressed by

$$R(\tau,x)=\begin{cases}Ke^{x+\mu_{\mathrm{Me}}+\frac{\sigma_{\mathrm{Me}}^2}{2}}\mathcal{N}\left(\frac{x-X_r+\mu_{\mathrm{Me}}+\sigma_{\mathrm{Me}}^2}{\sigma_{\mathrm{Me}}}\right)-Ke^{-r_I\tau}\mathcal{N}\left(\frac{x-X_r+\mu_{\mathrm{Me}}}{\sigma_{\mathrm{Me}}}\right) & \text{(Merton's)},\\ K\frac{a\eta_1}{\eta_1-1}e^{\eta_1 x+(1-\eta_1)X_r}-Kae^{-r_I\tau+\eta_1(x-X_r)} & \text{(Kou's)},\end{cases}$$

and for European put option by

$$R(\tau,x)=\begin{cases}Ke^{-r_I\tau}\mathcal{N}\left(\frac{X_l-x-\mu_{\mathrm{Me}}}{\sigma_{\mathrm{Me}}}\right)-Ke^{x+\mu_{\mathrm{Me}}+\frac{\sigma_{\mathrm{Me}}^2}{2}}\mathcal{N}\left(\frac{X_l-x-\mu_{\mathrm{Me}}-\sigma_{\mathrm{Me}}^2}{\sigma_{\mathrm{Me}}}\right) & \text{(Merton's)},\\ Kbe^{-r_I\tau+\eta_2(X_l-x)}-K\frac{b\eta_2}{\eta_2+1}e^{-\eta_2 x+(\eta_2+1)X_l} & \text{(Kou's)},\end{cases}$$

where $\mathcal{N}(x)$ is the cumulative normal distribution $\mathcal{N}(x)=\frac{1}{\sqrt{2\pi}}\int_{-\infty}^{x}e^{-\frac{\xi^2}{2}}d\xi$, which can be computed directly.

3. Abstract parabolic integro-differential equation. Let H and V be separable real Hilbert spaces with norms $|\cdot|$ and $\|\cdot\|$, respectively, such that V is densely and continuously embedded in H, which is equipped with the usual inner product $(\cdot,\cdot)$. Let V^* be the dual of V, and denote by $\|\cdot\|_*$ the dual norm on V^*. Then we have the Gelfand triple $V\subseteq H\subseteq V^*$. We still denote by $(\cdot,\cdot)$ the duality pairing between V^* and V. As a consequence, there exists a constant $\alpha>0$ such that

$$|v|\le\alpha\|v\|\quad\forall v\in V,\qquad \|f\|_*\le\alpha|f|\quad\forall f\in H. \tag{3.1}$$

Let us consider the abstract PIDE

$$u'(\tau)+\mathcal{A}u(\tau)+\mathcal{B}u(\tau)+\mathcal{J}(u(\tau))=F(\tau),\quad \tau\in(0,T], \tag{3.2}$$

$$u(0)=u^0, \tag{3.3}$$

where $\mathcal{A}:V\to V^*$ is defined via $(\mathcal{A}u,v)=a(u,v)$ by a continuous, strongly positive bilinear form $a(\cdot,\cdot):V\times V\to\mathbb{R}$, $F:(0,T]\to H$ and the initial data $u^0\in V$. Due to the properties of $a(\cdot,\cdot)$, we know that there exist constants $\beta\ge\mu>0$ with

$$|a(u,v)|\le\beta\|u\|\|v\|,\qquad a(v,v)\ge\mu\|v\|^2\quad\forall u,v\in V. \tag{3.4}$$

For the skew-symmetric part of $a(\cdot,\cdot)$, we assume

$$|a(u,v)-a(v,u)|\le\rho\|u\||v|\quad\forall u,v\in V, \tag{3.5}$$

with some $\rho\ge0$. If $a(\cdot,\cdot)$ is symmetric, we have $\rho=0$. For the linear operator $\mathcal{B}$, we assume that there exists a constant γ such that

$$|\mathcal{B}u|\le\gamma\|u\|\quad\forall u\in V. \tag{3.6}$$

It is easy to see that for option pricing problem (2.10), $\mathcal{L}$ is split into $\mathcal{A}$ and $\mathcal{B}$, with different choices for $\mathcal{A}$ and $\mathcal{B}$ as studied in [41]. For example, $\mathcal{A}$ ($\mathcal{B}=\mathcal{L}-\mathcal{A}$

accordingly) can be $-\frac{1}{2}\sigma^2\frac{\partial^2}{\partial x^2}+(\vartheta_1 r_I+\vartheta_2\lambda)I$ with $\vartheta_i\in[0,1]$, $i=1,2$. In all these cases, the operators $\mathcal{A}$ are sectorial, and the spectral theory of the operator $\mathcal{A}$ allows us to define the powers $\mathcal{A}^{\theta/2}$ of $\mathcal{A}$ for $\theta\in\mathbb{R}$ (see [48, 22]). For every $\theta>0$, $\mathcal{A}^{\theta/2}$ is an unbounded operator in H with a dense domain $\mathcal{D}(\mathcal{A}^{\theta/2})\subset H$. The space $\mathcal{D}(\mathcal{A}^{\theta/2})$, $0\le\theta\le 2$, is endowed with the norm $\|v\|_\theta:=|\mathcal{A}^{\theta/2}v|$. For $\theta=1$, we have $\mathcal{D}(\mathcal{A}^{1/2})=V$ and the equivalences of norms $|\mathcal{A}^{1/2}v|\approx\|v\|,\ v\in\mathcal{D}(\mathcal{A}^{1/2})$. From (3.4) and (3.1), we infer

$$\mu\|v\|^2\le a(v,v)=(\mathcal{A}v,v)\le\|\mathcal{A}v\|_*\|v\|\le\alpha|\mathcal{A}v|\|v\|,\quad v\in\mathcal{D}(\mathcal{A}),$$

and therefore,

$$\|v\|\le\frac{\alpha}{\mu}|\mathcal{A}v|=\frac{\alpha}{\mu}\|v\|_2. \tag{3.7}$$

The solution operator of the parabolic problem (3.2) generates an analytic semigroup $E(\tau)=\exp(-\tau\mathcal{A})$ (see, e.g., [22, 43]), and therefore the solution $u(\tau)$ becomes analytic with respect to τ in the open interval $(0,T]$. It follows from the analyticity that (with $D_t^l=\partial^l/\partial t^l, l=0,1,2,\dots$) [22]

$$|D_\tau^l E(\tau)v|=|\mathcal{A}^l E(\tau)v|\le C_l\tau^{-l}|v|,\quad 0<\tau\le 1,\ v\in H. \tag{3.8}$$

We use the ensuing smoothing property

$$\|D_\tau^l E(\tau)v\|_s\le C_l\tau^{-l-(s-\theta)/2}\|v\|_\theta,\quad \tau>0,\ v\in\mathcal{D}(\mathcal{A}^{\theta/2}),\quad 0\le\theta\le s\le 2,\ l=0,1. \tag{3.9}$$

As for the integral operator $\mathcal{J}$, we assume that it satisfies the condition

$$|\mathcal{J}u|\le C_J|u| \tag{3.10}$$

for some constant C_J independent of τ. As noted in [23], condition (3.10) is satisfied not only for a finite activity jump-diffusion model (e.g., Merton's model or Kou's model) but also for a more general jump-diffusion model, for example, CGMY or KoBoL (see [8, 11]) with infinite activity and finite variation.

Due to the nonsmoothness of the initial data u^0, singularities may arise at $\tau=0$. More specifically, we have the following time regularity result.

THEOREM 3.1 (time regularity). *Let $\mathfrak{B}\subset V$ be a bounded set, and let $0<\bar\tau\le T$ and $F\in C^2(0,T;H)$. If $u(\tau)\in\mathfrak{B}$ for $0\le\tau\le\min\{1,\bar\tau\}$, then*

$$\|u'(\tau)\|_\theta\le C(\mathfrak{B},\bar\tau)\tau^{-1-(\theta-1)/2},\qquad \tau\in(0,\bar\tau],\quad \theta\in[0,2), \tag{3.11}$$

$$|u^{(l)}(\tau)|\le C(\mathfrak{B},\bar\tau)\tau^{-l+1/2},\qquad \tau\in(0,\bar\tau],\quad l=1,2,3. \tag{3.12}$$

Proof. The proof will be based on the following generalization of Gronwall's lemma: if $\phi(\tau)$ satisfies

$$0\le\phi(\tau)\le G_1\tau^{-1+\alpha_1}+G_2\int_0^\tau(\tau-s)^{-1+\alpha_2}\phi(s)ds,\qquad \tau\in(0,\bar\tau], \tag{3.13}$$

then $\phi(\tau)\le C(G_2,\bar\tau,\alpha_1,\alpha_2)G_1\tau^{-1+\alpha_1}$ for $\tau\in(0,\bar\tau]$, provided that $G_i\ge 0$, $\alpha_i>0$, $i=1,2$ (see section 7.1 in [22] or Lemmas 6.3 and 7.1 in [15]). Then the assertion for

(3.11) and (3.12) with $l = 1$ can be proved by tracing the constants of Theorem 3.5.2 in [22]. To show that (3.12) holds for $l = 2$, we set $v_1(\tau) = \tau u'(\tau)$, which satisfies

$$v_1' + \mathcal{A}v_1 + \mathcal{B}v_1 + \mathcal{J}(v_1) = u' + \tau F', \quad \tau \in (0, \bar{\tau}]; \qquad v_1(0) = 0, \tag{3.14}$$

and therefore,

$$v_1(\tau) = \int_0^\tau E(\tau - s)\left[u'(s) + sF'(s) - \mathcal{B}v_1(s) - \mathcal{J}(v_1(s))\right] ds. \tag{3.15}$$

Then, in view of (3.9), (3.6), and (3.10),

$$\begin{aligned} \|v_1(\tau)\|_2 &\le C + C\int_0^\tau (\tau - s)^{-3/4}\|u'(s)\|_{1/2} ds + C\int_0^\tau (\tau - s)^{-1/2}\|v_1(s)\|_1 ds \\ &\le C(\mathfrak{B}, \bar{\tau})\tau^{-1/2} + C(\mathfrak{B})\int_0^\tau (\tau - s)^{-1/2}\|v_1(s)\|_2 ds. \end{aligned} \tag{3.16}$$

Using the generalization of Gronwall's lemma (3.13), we get

$$\|v_1(\tau)\|_2 \le C(\mathfrak{B}, \bar{\tau})\tau^{-1/2}, \tag{3.17}$$

and therefore, using (3.14), (3.7), and (3.12) with $l = 1$ just proved,

$$\begin{aligned} |v_1'(\tau)| &= |\mathcal{A}v_1 + \mathcal{B}v_1 + \mathcal{J}(v_1) - u' - \tau F'| \\ &\le \left(1 + \frac{\alpha\gamma}{\mu}\right)\|v_1(\tau)\|_2 + C_J|v_1(\tau)| + |u'| + \tau|F'| \le C(\mathfrak{B}, \bar{\tau})\tau^{-1/2}, \end{aligned} \tag{3.18}$$

which implies the desired estimate (3.12) with $l = 2$.

To show that (3.12) holds for $l = 3$, we show a more general result than (3.18) for v_1'. For this purpose, we use Lemma 3.5.1 in [22] as follows: if $\mathcal{A}$ is a sectorial operator, and $\psi : (0, T) \to \mathcal{D}(\mathcal{A})$ satisfies $|\psi(t) - \psi(s)| \le \bar{\psi}(s)(t - s)$, $0 < s < t < T$, with $\bar{\psi}(\cdot)$ being continuous on interval $(0, T)$ and $\int_0^T \bar{\psi}(s)ds < \infty$, then for $0 \le \theta < 2$, $\Psi(t) \equiv \int_0^t E(t-s)\psi(s)ds$ $(0 < t < T)$: $(0, T) \to \mathcal{D}(\mathcal{A}^{\theta/2})$ is continuously differentiable, and

$$\|\Psi'(t)\|_\theta \le Ct^{-\theta/2}|\psi(t)| + C\int_0^t (t - s)^{-\theta/2}\bar{\psi}(s)ds, \tag{3.19}$$

where C is a constant independent of θ and ψ. It is easy to obtain from (3.18) and (3.12) with $l = 2$ that for $s < \tau$,

$$\begin{aligned} &|u'(\tau) + \tau F'(\tau) - \mathcal{B}v_1(\tau) - \mathcal{J}(v_1(\tau)) - u'(s) - sF'(s) + \mathcal{B}v_1(s) + \mathcal{J}(v_1(s))| \\ &\quad \le \max_{s\le t\le\tau} |u^{(2)}(t)|(\tau - s) + C(\tau - s) + (\gamma + C_J)\max_{s\le t\le\tau} |v_1'(t)|(\tau - s) \\ &\quad \le C(\mathfrak{B}, \bar{\tau})s^{-3/2}(t - s). \end{aligned} \tag{3.20}$$

As a consequence of (3.19), for $0 \le \theta < 1$ we obtain

$$\begin{aligned} \|v_1'(\tau)\|_\theta &= \left\| \frac{d}{d\tau}\int_0^\tau E(\tau - s)\left[u'(s) + sF'(s) - \mathcal{B}v_1(s) - \mathcal{J}(v_1(s))\right] ds \right\|_\theta \\ &\le C\tau^{-\frac{\theta}{2}}|u'(\tau) + \tau F'(\tau) - \mathcal{B}v_1(\tau) - \mathcal{J}(v_1(\tau))| + C\int_0^\tau (\tau - s)^{-\theta/2}s^{-3/2} ds \\ &\le C\tau^{-\frac{\theta+1}{2}}. \end{aligned} \tag{3.21}$$

Now let $v_2(\tau) = \tau^2 u''(\tau)$. Similarly, it satisfies

$$v_2' + \mathcal{A}v_2 + \mathcal{B}v_2 + \mathcal{J}(v_2) = 2\tau u'' + \tau^2 F'', \quad \tau \in (0, \bar{\tau}]; \quad v_2(0) = 0. \tag{3.22}$$

Hence,

$$v_2(\tau) = \int_0^\tau E(\tau - s)\left[2su''(s) + s^2 F''(s) - \mathcal{B}v_2(s) - \mathcal{J}(v_2(s))\right] ds. \tag{3.23}$$

In view of $su''(s) = v_1'(s) - u'$, using (3.9), we have

$$\begin{aligned} \|v_2(\tau)\|_2 &\le C\int_0^\tau (\tau - s)^{-3/4}\|v_1'(\tau)\|_{1/2} ds + C\int_0^\tau (\tau - s)^{-3/4}\|u'(s)\|_{1/2} ds \\ &\quad + C + C\int_0^\tau (\tau - s)^{-1/2}\|v_2\|_1 ds \\ &\le C\tau^{-1/2} + C\int_0^\tau (\tau - s)^{-1/2}\|v_2\|_2 ds. \end{aligned} \tag{3.24}$$

Hence an application of the generalization of Gronwall's lemma (3.13) yields

$$\|v_2(\tau)\|_2 \le C\tau^{-1/2}, \tag{3.25}$$

which implies $|v_2'(\tau)| \le C\tau^{-1/2}$. Then the desired estimate (3.12) with $l = 3$ follows from $v_2'(\tau) = 2\tau u^{(2)}(\tau) + \tau^2 u^{(3)}(\tau)$, and the proof is completed. ∎

4. Stability and convergence of time semidiscrete scheme. In this section, we will study the stability, consistency, and convergence of the variable step-size IMEX BDF2 method for abstract PIDE (3.2).

4.1. The variable step-size IMEX BDF2 time discretization. Let the time interval $[0, T]$ for given $N \in \mathbb{N}$, $N \ge 2$, be partitioned via $J^N : 0 = \tau_0 < \tau_1 < \cdots < \tau_N = T$. Let $k_n = \tau_n - \tau_{n-1}$, $n = 1, 2, \ldots, N$, be the time step-sizes which in general will be variable, and $J_n := (\tau_{n-1}, \tau_n]$, $n = 1, 2, \ldots, N$. We set

$$r_n = \frac{k_n}{k_{n-1}}, \quad n = 2, 3, \ldots, N; \quad k_{\max} = \max_{n=1,2,\ldots,N} k_n; \quad r_{\max} = \max\left(\max_{n=2,\ldots,N} r_n, 1\right).$$

Let us use the notation $u^n := u^n(x)$ to denote the approximation of $u(\tau_n, x)$, and define $Eu^{n-1} = (1 + r_n)u^{n-1} - r_n u^{n-2}$ and

$$\bar{\partial}_B^2 u^n = \frac{1}{k_n}\Big((1 + s_n)u^n - (1 + r_n)u^{n-1} + r_n s_n u^{n-2}\Big), \tag{4.1}$$

where $s_n := \frac{r_n}{1+r_n}$. Then (3.2) will be discretized by the variable step-size IMEX BDF2 scheme,

$$\bar{\partial}_B^2 u^n + \mathcal{A}u^n + \mathcal{B}_1 u^n + \mathcal{B}_2 Eu^{n-1} + \mathcal{J}(Eu^{n-1}) = F^n, \quad n \ge 2, \tag{4.2}$$

together with an appropriate boundary condition resulting from (2.8) and (2.9), where $F^n := F(\tau_n)$ and $\mathcal{B}_1 + \mathcal{B}_2 = \mathcal{B}$. For example, for the call option, from (2.8) we have the boundary condition

$$u^n(X_l) = 0 \quad \text{and} \quad u^n(X_r) = e^{X_r} - Ke^{-r_I \tau_n}. \tag{4.3}$$

The value u^0 at the zeroth time level is given by an initial condition of the model problem, and the start value u^1 can be obtained by applying the IMEX Euler scheme of order one,

$$\bar{\partial}_B^1 u^1 + \mathcal{A}_1 u^1 + \mathcal{B}_1 u^1 + \mathcal{B}_2 u^0 + \mathcal{J}(u^0) = F^1, \tag{4.4}$$

together with an appropriate boundary condition, where $\bar{\partial}_B^1 u^n := \frac{u^n - u^{n-1}}{k_n}$.

We conclude this subsection with a few remarks about the scheme (4.2).

We first remark that with the backward divided difference $\bar{\partial}_B^1 u^n$, $\bar{\partial}_B^2 u^n$ can be expressed by

$$\bar{\partial}_B^2 u^n = \frac{1+2r_n}{1+r_n}\bar{\partial}_B^1 u^n - \frac{r_n}{1+r_n}\bar{\partial}_B^1 u^{n-1} = (1+s_n)\bar{\partial}_B^1 u^n - s_n \bar{\partial}_B^1 u^{n-1},$$

and for an equidistant partition with $k_n \equiv k$, we have the well-known formula

$$\bar{\partial}_B^2 u^n = \frac{1}{k}\Big(\frac{3}{2}u^n - 2u^{n-1} + \frac{1}{2}u^{n-2}\Big). \tag{4.5}$$

It is also noteworthy that $\bar{\partial}_B^2$ formally degenerates to $\bar{\partial}_B^1$, and the variable step-size IMEX BDF2 scheme (4.2) degenerates to the variable step-size IMEX Euler scheme whenever $r_n = 0$.

Our second remark is about the operator splitting $\mathcal{B} = \mathcal{B}_1 + \mathcal{B}_2$. Motivated by the interesting results obtained in [41] on IMEX schemes with a convex combination parameter $c \in [0,1]$, which divides the zero-order term λu due to the jumps between the implicit and explicit parts, we consider a more general IMEX scheme with operator splitting $\mathcal{B} = \mathcal{B}_1 + \mathcal{B}_2$, where we treat $\mathcal{B}_1 u$ implicitly and $\mathcal{B}_2 u$ explicitly. As done for $\mathcal{B}$, we assume that

$$|\mathcal{B}_i u| \le \gamma_i \|u\| \quad \forall u \in V, \quad i = 1, 2, \tag{4.6}$$

with $\gamma_i \ge 0$, $i = 1, 2$.

4.2. Stability of IMEX-BDF2 scheme for abstract PIDE. To study the stability of the IMEX-BDF2 scheme, let us consider the perturbed equation

$$\bar{\partial}_B^2 \tilde{u}^n + \mathcal{A}\tilde{u}^n + \mathcal{B}_1 \tilde{u}^n + \mathcal{B}_2 E\tilde{u}^{n-1} + \mathcal{J}(E\tilde{u}^{n-1}) = F^n + \xi^n, \quad n \ge 2, \tag{4.7}$$

together with the same boundary condition as in (4.2). We also consider the perturbed equation

$$\bar{\partial}_B^1 \tilde{u}^1 + \mathcal{A}\tilde{u}^1 + \mathcal{B}_1 \tilde{u}^1 + \mathcal{B}_2 \tilde{u}^0 + \mathcal{J}(\tilde{u}^0) = F^1 + \xi^1, \tag{4.8}$$

together with the same boundary condition as in (4.4). The ξ^n is the perturbation in the data at any time level τ_n, and we will examine the effect of these perturbations on the error as we proceed in time. Let us define the error term $\varepsilon^n := \tilde{u}^n - u^n$. The error term ε^n will be zero at the boundary points since the boundary conditions in equations (4.2) (respectively, (4.4)) and perturbed equations (4.7) (respectively, (4.8)) are exactly same.

To prove the stability of the variable step-size IMEX BDF2 scheme, we need the following discrete Gronwall lemma proved in [16].

LEMMA 4.1 (discrete Gronwall lemma [16]). *Let* $a_n,\ b_n,\ c_n,\ \lambda_n \geq 0$ *with* $\{c_n\}$ *monotonically increasing, and let* $0 \leq \varpi < 1$. *Then*

$$a_n + b_n \leq \sum_{j=2}^{n-1} \lambda_j a_j + \varpi a_n + c_n, \qquad n = 2, 3, \ldots, \tag{4.9}$$

implies for $n = 2, 3, \ldots,$

$$a_n + b_n \leq \frac{c_n}{1-\varpi} \prod_{j=2}^{n-1} \left(1 + \frac{\lambda_j}{1-\varpi}\right) \leq \frac{c_n}{1-\varpi} \exp\left(\frac{1}{1-\varpi} \sum_{j=2}^{n-1} \lambda_j\right).$$

We now present the stability result.

THEOREM 4.2 (stability). *Let* $r_{\max} \leq R$ *with* $1 < R < \bar{R} \approx 1.91$, *with* $\bar{R}$ *a root of*

$$\chi(R) := (R+1)^4 - R(R-1)^2(3R+1)^2.$$

Then for sufficiently small step-sizes $0 < k_n \leq k_{\max}$, *the following estimate holds for* $n = 2, 3, \ldots, N$:

$$|\varepsilon^n| \leq C \left(|\varepsilon^0| + k_1(\|\varepsilon^1\| + \|\varepsilon^0\|) + \sum_{j=1}^{n} k_j |\xi^j| \right). \tag{4.10}$$

Here C *depends on the constants in* (3.1), (3.4)–(3.10), *and* R, T, Φ_n, *with* Φ_n *defined by*

$$\Phi_n := \sum_{j=2}^{n-2} [r_j - r_{j+2}]_+, \qquad [a]_+ := \frac{|a| + a}{2}.$$

Proof. The idea of the proof stems from [16]. We first set

$$\varepsilon_\delta^n = \varepsilon^n + \delta(\varepsilon^n - \varepsilon^{n-1}) = (1+\delta)\varepsilon^n - \delta\varepsilon^{n-1}. \tag{4.11}$$

Subtracting (4.2) from (4.7), we obtain

$$\bar{\partial}_B^2 \varepsilon^n + \mathcal{A}\varepsilon^n + \mathcal{B}_1 \varepsilon^n + \mathcal{B}_2 E\varepsilon^{n-1} + \mathcal{J}(E\varepsilon^{n-1}) = \xi^n, \quad n \geq 2. \tag{4.12}$$

Taking in (4.12) the inner product with $\frac{2k_n}{1+r_n}\varepsilon_\delta^n$ yields

$$\begin{aligned} &\frac{2k_n}{1+r_n}\left(\bar{\partial}_B^2 \varepsilon^n, \varepsilon_\delta^n\right) + \frac{2k_n}{1+r_n} a\left(\varepsilon^n, \varepsilon_\delta^n\right) + \frac{2k_n}{1+r_n}\left(\mathcal{B}_1 \varepsilon^n, \varepsilon_\delta^n\right) + \frac{2k_n}{1+r_n}\left(\mathcal{B}_2 E\varepsilon^{n-1}, \varepsilon_\delta^n\right) \\ &+ \frac{2k_n}{1+r_n}\left(\mathcal{J}(E\varepsilon^{n-1}), \varepsilon_\delta^n\right) = \frac{2k_n}{1+r_n}\left(\xi^n, \varepsilon_\delta^n\right), \qquad n = 2, 3, \ldots, N. \end{aligned} \tag{4.13}$$

Then we estimate each term of (4.13). The first term on the left-hand side of (4.13) can be estimated as

$$\begin{aligned} \frac{2k_n}{1+r_n}(\bar{\partial}_B^2 \varepsilon^n, \varepsilon_\delta^n) &= \frac{k_n}{1+r_n}\bar{\partial}_B^2 |\varepsilon^n|^2 + A_\delta(r_n)|\varepsilon^n - \varepsilon^{n-1}|^2 - B_\delta(r_n)|\varepsilon^{n-1} - \varepsilon^{n-2}|^2 \\ &\quad + (1+\delta)s_n^2 |\varepsilon^n - 2\varepsilon^{n-1} + \varepsilon^{n-2}|, \end{aligned} \tag{4.14}$$

where

$$A_\delta(r_n)=\frac{1+2r_n-r_n^2+\delta(2+4r_n-r_n^2)}{(1+r_n)^2},\quad B_\delta(r_n)=(2+\delta)s_n^2.$$

Summation gives

$$\begin{aligned}2\sum_{j=2}^{n}\frac{k_j}{1+r_j}(\bar\partial_B^2\varepsilon^j,\varepsilon_\delta^j)&=\sum_{j=2}^{n}\frac{k_j}{1+r_j}\bar\partial_B^2|\varepsilon^j|^2+A_\delta(r_n)|\varepsilon^n-\varepsilon^{n-1}|^2\\&\quad+\sum_{j=2}^{n-1}(A_\delta(r_j)-B_\delta(r_{j+1}))|\varepsilon^j-\varepsilon^{j-1}|^2-B(r_2)|u^1-u^0|^2\\&\quad+(1+\delta)\sum_{j=2}^{n}\frac{k_j}{1+r_j}s_j^2|\varepsilon^j-2\varepsilon^{j-1}+\varepsilon^{j-2}|.\end{aligned}\tag{4.15}$$

Taking into account that $A_\delta(r)$ is a decreasing function and $B_\delta(r)$ is an increasing function, we have

$$A_\delta(r_j)-B_\delta(r_{j+1})\ge A_\delta(R)-B_\delta(R)=\frac{1+2R-3R^2+2\delta(1+2R-R^2)}{(1+R)^2}.\tag{4.16}$$

Choosing

$$\hat\delta=\hat\delta(R)=\frac{-1}{2}\frac{1+2R-3R^2}{1+2R-R^2}=-\frac{3(R-1)(R+\frac{1}{3})}{2(R-1-\sqrt{2})(R-1+\sqrt{2})},$$

we have $A_\delta(r_j)-B_\delta(r_{j+1})\ge 0$, and for $1<R<\bar R$,

$$\frac{1}{2}<A_\delta(R)=B_\delta(R)=\frac{R^2(R-3-2\sqrt{3})(R-3+2\sqrt{3})}{2(1+R)^2(R-1-\sqrt{2})(R-1+\sqrt{2})}<2.\tag{4.17}$$

The first term on the right-hand side of (4.15) can be reformulated as

$$\begin{aligned}\sum_{j=2}^{n}\frac{k_j}{1+r_j}\bar\partial_B^2|\varepsilon^j|^2&=\frac{1+2r_n}{(1+r_n)^2}|\varepsilon^n|^2-s_{n-1}^2|\varepsilon^{n-1}|^2+\sum_{j=2}^{n-2}\left(\frac{1+2r_j}{(1+r_j)^2}-1+s_{j+2}^2\right)|\varepsilon^j|^2\\&\quad-\frac{1+2r_3}{(1+r_3)^2}|\varepsilon^1|^2+s_2^2|\varepsilon^0|^2.\end{aligned}\tag{4.18}$$

Since the nonnegative function $\frac{d}{dr}(r^2/(1+r)^2)$ takes its maximum value $8/27$ at $r=1/2$, we have

$$\frac{1+2r_j}{(1+r_j)^2}-1+s_{j+2}^2=s_{j+2}^2-s_j^2\ge-\frac{8}{27}[r_j-r_{j+2}]_+.\tag{4.19}$$

Substituting (4.16), (4.17), (4.18), and (4.19) into (4.15), considering $\varepsilon^0=0$, we obtain

$$\begin{aligned}2\sum_{j=2}^{n}\frac{k_j}{1+r_j}(\bar\partial_B^2\varepsilon^j,\varepsilon_{\hat\delta}^j)&\ge\frac{1+2R}{(1+R)^2}|\varepsilon^n|^2-\frac{R^2}{(1+R)^2}|\varepsilon^{n-1}|^2+\frac{1}{2}|\varepsilon^n-\varepsilon^{n-1}|^2\\&\quad-\left(3|\varepsilon^1|^2+\sum_{j=2}^{n-2}\frac{8}{27}[r_j-r_{j+2}]_+|\varepsilon^j|^2\right)\\&\quad+(1+\hat\delta)\sum_{j=2}^{n}\frac{k_j}{1+r_j}s_j^2|\varepsilon^j-2\varepsilon^{j-1}+\varepsilon^{j-2}|.\end{aligned}\tag{4.20}$$

Using (3.5) and Young's inequality, we find

$$\delta|a(\varepsilon_\delta^n,\varepsilon^{n-1})-a(\varepsilon^{n-1},\varepsilon_\delta^n)|\le\delta\rho\|\varepsilon_\delta^n\||\varepsilon^{n-1}|\le\frac{1}{2}a(\varepsilon_\delta^n,\varepsilon_\delta^n)+\frac{\delta^2\rho^2}{2\mu}|\varepsilon^{n-1}|^2. \tag{4.21}$$

Then $2a(\varepsilon^n,\varepsilon_\delta^n)$ in the second term on the left-hand side of (4.13) can be estimated by

$$\begin{aligned}2a(\varepsilon^n,\varepsilon_\delta^n)\ge{}&\frac{1}{2(1+\delta)}a(\varepsilon_\delta^n,\varepsilon_\delta^n)+(1+\delta)a(\varepsilon^n,\varepsilon^n)-\frac{\delta^2}{1+\delta}a(\varepsilon^{n-1},\varepsilon^{n-1})\\&-\frac{\delta^2\rho^2}{2\mu(1+\delta)}|\varepsilon^{n-1}|^2.\end{aligned} \tag{4.22}$$

Now we estimate the third and fourth terms on the left-hand side of (4.13). With (4.6), for sufficiently small $\epsilon_i>0$, $i=1,2,3$, we get

$$2|(\mathcal{B}_1\varepsilon^n,\varepsilon_\delta^n)|\le2\gamma_1\|\varepsilon^n\||\varepsilon_\delta^n|\le\epsilon_1a(\varepsilon^n,\varepsilon^n)+\frac{\gamma_1^2}{\epsilon_1\mu}|\varepsilon_\delta^n|^2 \tag{4.23}$$

and

$$\begin{aligned}2|(\mathcal{B}_2E\varepsilon^{n-1},\varepsilon_\delta^n)|&\le2\gamma_2(1+r_n)\|\varepsilon^{n-1}\||\varepsilon_\delta^n|+2\gamma_2r_n\|\varepsilon^{n-2}\||\varepsilon_\delta^n|\\&\le\epsilon_2a(\varepsilon^{n-1},\varepsilon^{n-1})+\epsilon_3a(\varepsilon^{n-2},\varepsilon^{n-2})+\left(\frac{(1+r_n)^2\gamma_2^2}{\epsilon_2\mu}+\frac{r_n^2\gamma_2^2}{\epsilon_3\mu}\right)|\varepsilon_\delta^n|^2.\end{aligned} \tag{4.24}$$

The fifth term on the left-hand side of (4.13) can be bounded by

$$\begin{aligned}2|(\mathcal{J}(E\varepsilon^{n-1}),\varepsilon_\delta^n)|&\le\frac{2\alpha^2C_J^2(1+\delta)}{\mu}|E\varepsilon^{n-1}|^2+\frac{\mu}{2(1+\delta)}\|\varepsilon_\delta^n\|^2\\&\le\frac{4\alpha^2C_J^2(1+\delta)}{\mu}\left[(1+r_n)^2|\varepsilon^{n-1}|^2+r_n^2|\varepsilon^{n-2}|^2\right]\\&\quad+\frac{1}{2(1+\delta)}a(\varepsilon_\delta^n,\varepsilon_\delta^n).\end{aligned} \tag{4.25}$$

The term on the right-hand side of (4.13) can be bounded by

$$2|(\xi^n,\varepsilon_\delta^n)|\le2|\xi^n||\varepsilon_\delta^n|\le2(1+\delta)|\xi^n|\left(|\varepsilon^n|+|\varepsilon^{n-1}|\right). \tag{4.26}$$

Noting that

$$|\varepsilon_\delta^n|^2\le2\max\{1,\delta^2\}\left(|\varepsilon^n|^2+|\varepsilon^n-\varepsilon^{n-1}|^2\right)\le C_\delta\left(|\varepsilon^n|^2+|\varepsilon^{n-1}|^2\right), \tag{4.27}$$

with (4.20) and (4.22)–(4.26), we obtain

$$
\begin{aligned}
&\frac{1+2R}{(1+R)^2}|\varepsilon^n|^2-\frac{R^2}{(1+R)^2}|\varepsilon^{n-1}|^2+\frac{1}{2}|\varepsilon^n-\varepsilon^{n-1}|^2+\frac{k_n(1+\hat{\delta})}{1+r_n}a(\varepsilon^n,\varepsilon^n)\\
&+\sum_{j=2}^{n-1}\frac{k_j}{1+r_j}\left[1+\hat{\delta}-\epsilon_1-\left(\frac{\hat{\delta}^2}{1+\hat{\delta}}+\epsilon_2\right)s_{j+1}(1+r_j)-\epsilon_3 s_{j+2}r_{j+1}(1+r_j)\right]a(\varepsilon^j,\varepsilon^j)\\
&\le 3|\varepsilon^1|^2+\frac{\hat{\delta}^2}{1+\hat{\delta}}\frac{k_2}{1+r_2}a(\varepsilon^1,\varepsilon^1)+\sum_{j=2}^{n-2}\frac{8}{27}[r_{j+2}-r_j]_-|\varepsilon^j|^2\\
&\quad+\frac{\hat{\delta}^2\rho^2}{2\mu(1+\hat{\delta})}\sum_{j=2}^{n}\frac{k_j}{1+r_j}|\varepsilon^{j-1}|^2+\sum_{j=2}^{n}\frac{2(1+\hat{\delta})k_j}{1+r_j}|\xi^j|\left(|\varepsilon^j|+|\varepsilon^{j-1}|\right)\\
&\quad+\frac{C_\delta}{\mu}\sum_{j=2}^{n}\frac{k_j}{1+r_j}\left(\frac{\gamma_1^2}{\epsilon_1}+\frac{(1+r_j)^2\gamma_2^2}{\epsilon_2}+\frac{r_j^2\gamma_2^2}{\epsilon_3}\right)\left(|\varepsilon^j|^2+|\varepsilon^{j-1}|^2\right)\\
&\quad+\frac{4\alpha^2C_J^2(1+\hat{\delta})}{\mu}\sum_{j=1}^{n}\frac{k_j(1+2r_j+2r_j^2)}{1+r_j}|\varepsilon^{j-1}|^2.
\end{aligned}
\tag{4.28}
$$

In view of $s_{j+1}(1+r_j)\le R$ and $s_{j+2}r_{j+1}(1+r_j)\le R^2$, to prove the stability result, we should choose ϵ_i, $i=1,2,3$, such that

$$
1+\hat{\delta}-\epsilon_1-\left(\frac{\hat{\delta}^2}{1+\hat{\delta}}+\epsilon_2\right)R-\epsilon_3R^2\ge 0. \tag{4.29}
$$

Condition (4.29) requires

$$
R<\left(\frac{1+\hat{\delta}}{\hat{\delta}}\right)^2=\frac{(R+1)^4}{(R-1)^2(3R+1)^2}, \tag{4.30}
$$

which is equivalent to $\chi(R)>0$. Using $1<R<\bar{R}$, from (4.28), we obtain

$$
\begin{aligned}
\frac{1+2R}{(1+R)^2}|\varepsilon^n|^2\le\frac{R^2}{(1+R)^2}|\varepsilon^{n-1}|^2+c_1\Bigg[&\left(\frac{\rho^2+\alpha^2C_J^2}{\mu}+C_\epsilon\right)\sum_{j=3}^{n-1}k_j|\varepsilon^j|^2\\
&+C_\epsilon k_n\left(|\varepsilon^n|^2+|\varepsilon^{n-1}|^2\right)+|\varepsilon^1|^2+k_2\|\varepsilon^1\|^2\\
&+\sum_{j=2}^{n-2}[r_j-r_{j+2}]_+|\varepsilon^j|^2+\sum_{j=2}^{n}k_j|\xi^j|\left(|\varepsilon^j|+|\varepsilon^{j-1}|\right)\Bigg],
\end{aligned}
\tag{4.31}
$$

where

$$
C_\epsilon:=\frac{C_\delta}{\mu}\left(\frac{\gamma_1^2}{\epsilon_1}+\frac{\gamma_2^2}{\epsilon_2}+\frac{\gamma_2^2}{\epsilon_3}\right).
$$

Subtracting (4.4) from (4.8), we obtain

$$
\bar{\partial}_B^1\varepsilon^1+\mathcal{A}\varepsilon^1+\mathcal{B}_1\varepsilon^1+\mathcal{B}_2\varepsilon^0+\mathcal{J}(\varepsilon^0)=\xi^1. \tag{4.32}
$$

Take in (4.32) the inner product with $k_1\varepsilon^1$ to obtain

$$
\begin{aligned}
&\frac{1}{2}\left(|\varepsilon^1|^2-|\varepsilon^0|^2+|\varepsilon^1-\varepsilon^0|^2\right)+\mu k_1\|\varepsilon^1\|^2\\
&\le\gamma_1k_1\|\varepsilon^1\||\varepsilon^1|+\gamma_2k_1\|\varepsilon^0\||\varepsilon^1|+C_Jk_1|\varepsilon^0||\varepsilon^1|+k_1|\xi^1||\varepsilon^1|,
\end{aligned}
\tag{4.33}
$$

which implies

$$|\varepsilon^1|^2 + k_2\|\varepsilon^1\|^2 \le C|\varepsilon^0|^2 + Ck_1\left(\|\varepsilon^1\||\varepsilon^1| + \|\varepsilon^0\||\varepsilon^1| + |\varepsilon^0||\varepsilon^1| + |\xi^1||\varepsilon^1|\right). \tag{4.34}$$

Let $n^* = n^*(n)$ be such that $|\varepsilon^{n^*}| = \max_{l=1,\dots,n}|\varepsilon^l|$ for $n = 2, 3, \dots, N$. Substitute (4.34) into (4.31) and consider it with n replaced by n^*. This allows us to cancel a factor $|\varepsilon^{n^*}|$ so that

$$\frac{1+2R}{(1+R)^2}|\varepsilon^{n^*}| \le \frac{R^2}{(1+R)^2}|\varepsilon^{n^*-1}| + Q_{n^*}, \tag{4.35}$$

with

$$\begin{aligned} Q_n = c_2 \Bigg[&\left(\frac{\rho^2+\alpha^2C_J^2}{\mu} + C_\epsilon\right)\sum_{j=3}^{n-1} k_j|\varepsilon^j| + C_\epsilon k_n\left(|\varepsilon^n| + |\varepsilon^{n-1}|\right) + |\varepsilon^0| \\ &+ k_1(\|\varepsilon^1\| + \|\varepsilon^0\|) + \sum_{j=2}^{n-2}[r_j - r_{j+2}]_+|\varepsilon^j| + \sum_{j=1}^{n} k_j|\xi^j| \Bigg]. \end{aligned} \tag{4.36}$$

As an important step, we show

$$|\varepsilon^n| \le c_3 Q_n. \tag{4.37}$$

To do this, we first observe that for $n^* = 1$,

$$|\varepsilon^{n^*}| \le \frac{(1+R)^2}{1+2R-R^2}Q_n. \tag{4.38}$$

Now we show that (4.38) is valid for $n^* \ge 2$. Due to $Q_{n^*} \le Q_n$, it follows from (4.35) with $n^* = n$ that

$$\frac{1+2R}{(1+R)^2}|\varepsilon^{n^*}| \le \frac{R^2}{(1+R)^2}|\varepsilon^{n^*-1}| + Q_{n^*} \le \frac{R^2}{(1+R)^2}|\varepsilon^{n^*-1}| + Q_n. \tag{4.39}$$

Since $R < \bar{R} \approx 1.91$, (4.39) implies (4.38). Combining (4.35) and (4.38), we have

$$\frac{1+2R}{(1+R)^2}|\varepsilon^n| \le \left(\frac{R^2}{1+2R-R^2} + 1\right)Q_n = \frac{1+2R}{1+2R-R^2}Q_n. \tag{4.40}$$

Then (4.37) follows from $1 < R < \bar{R} \approx 1.91$.

When $k_{\max}$ is sufficiently small such that $c_3c_2C_\epsilon k_{\max} < \frac{1}{2}$, by Lemma 4.1 we have

$$|\varepsilon^n| \le 2c_2c_3E_n\left(|\varepsilon^0| + k_1(\|\varepsilon^1\| + \|\varepsilon^0\|) + \sum_{j=1}^{n} k_j|\xi^j|\right), \tag{4.41}$$

where

$$\begin{aligned} E_n &= \left[1 + 2c_2c_3\left(\frac{\rho^2+\alpha^2C_J^2}{\mu} + 2C_\varepsilon\right)k_n\right] \\ &\quad \times \prod_{j=2}^{n-2}\left[1 + 2c_2c_3[r_j - r_{j+2}]_+ + 2c_2c_3\left(\frac{\rho^2+\alpha^2C_J^2}{\mu} + C_\varepsilon\right)k_{j+1}\right] \\ &\le \exp\left(2c_2c_3\Phi_n + 2c_2c_3\left(\frac{\rho^2+\alpha^2C_J^2}{\mu} + 2C_\varepsilon\right)t_n\right). \end{aligned} \tag{4.42}$$

This completes the proof. ∎

Remarks. (1) We find that the larger the admissible step-size $k_{\max}$, the smaller the admissible step-size ratio $r_{\max}$. The relationship can be observed from the conditions (4.29) and $c_3c_2C_\epsilon k_{\max} < \frac{1}{2}$.

(2) We observe that the splitting $\mathcal{B} = \mathcal{B}_1 + \mathcal{B}_2$ has little influence on the choice of the step-sizes k_n, that is, the step-size restriction for treating $\mathcal{B}_2 u$ explicitly is practically identical to that for treating $\mathcal{B}_2 u$ implicitly.

4.3. Consistency error. Let $u(\tau_n)$ denote the nodal values of the exact solution $u(\tau)$. The consistency error d^n of the schemes (4.2) for the solution u of (3.2), i.e., the amounts by which the exact solution misses satisfying (4.2), is given by

$$d^n = \bar{\partial}_B^2 u(\tau_n) + \mathcal{A}u(\tau_n) + \mathcal{B}_1 u(\tau_n) + \mathcal{B}_2 Eu(\tau_{n-1}) + \mathcal{J}(Eu(\tau_{n-1})) - F(\tau_n), \quad n = 2, \ldots, N. \tag{4.43}$$

It follows from (3.2) and (4.2) that

$$d^n = \bar{\partial}_B^2 u^n - u'(\tau_n) + \mathcal{B}_2(\tilde{d}_2^n) + \mathcal{J}(\tilde{d}_2^n), \tag{4.44}$$

where $\tilde{d}_2^n = Eu(\tau_{n-1}) - u(\tau_n)$. By Taylor expanding about τ_{n-1}, we obtain

$$\tilde{d}_2^n = \int_{\tau_{n-1}}^{\tau_n} (\tau_n - \tau) u''(\tau) d\tau + r_n \int_{\tau_{n-2}}^{\tau_{n-1}} (\tau - \tau_{n-2}) u''(\tau) d\tau. \tag{4.45}$$

Furthermore, for $n \geq 2$ we obtain

$$\begin{aligned} d^n = {} & \frac{(1+r_n)}{2k_n} \int_{\tau_{n-1}}^{\tau_n} (\tau_{n-1} - \tau)^2 u'''(\tau) d\tau - \frac{r_n s_n}{2k_n} \int_{\tau_{n-2}}^{\tau_n} (\tau - \tau_{n-2})^2 u'''(\tau) d\tau \\ & + \mathcal{B}_2(\tilde{d}_2^n) + \mathcal{J}(\tilde{d}_2^n). \end{aligned} \tag{4.46}$$

As mentioned in section 2, $\bar{\partial}_B^2$ degenerate to $\bar{\partial}_B^1$ whenever $r_n = 0$. In this case, we come up with

$$\tilde{d}_2^n := u(\tau_n) - u(\tau_{n-1}) = \int_{\tau_{n-1}}^{\tau_n} u'(\tau) d\tau \tag{4.47}$$

and

$$\begin{aligned} d^n &= \bar{\partial}_B^1 u^n - u'(t_n) + \mathcal{B}_2(\tilde{d}_2^n) + \mathcal{J}(\tilde{d}_2^n) \\ &= -\frac{1}{k_n} \int_{\tau_{n-1}}^{\tau_n} (\tau - \tau_{n-1}) u''(\tau) d\tau + \mathcal{B}_2(\tilde{d}_2^n) + \mathcal{J}(\tilde{d}_2^n). \end{aligned} \tag{4.48}$$

The consistency errors of these schemes can be bounded by the following lemma.

LEMMA 4.3. *Let $\mathfrak{B} \subset V$ be a bounded set, and let $0 < T < 1$. If $u(\tau) \in \mathfrak{B}$ for $0 \leq \tau \leq T$, then the consistency error* (4.46) *of the IMEX BDF2 scheme is bounded by*

$$|d^n| \leq C\left(k_n^2 \tau_{n-1}^{-5/2} + k_n k_{n-1} \tau_{n-2}^{-5/2}\right) + C\left(k_n^2 \tau_{n-1}^{-3/2} + k_n k_{n-1} \tau_{n-2}^{-3/2}\right), \ n \geq 3. \tag{4.49}$$

The consistency error (4.48) *of the IMEX Euler scheme is bounded by*

$$|d^n| \leq C k_n \left(\tau_{n-1}^{-3/2} + \tau_{n-1}^{-1/2}\right), \qquad n \geq 2. \tag{4.50}$$

Proof. We first focus on the IMEX BDF2 scheme. Under the assumptions of the theorem, we bound $\tilde{d}_2^n$, $n \geq 3$, as follows using Theorem 3.1:

$$|\tilde{d}_2^n| = \left| \int_{\tau_{n-1}}^{\tau_n} (\tau_n - \tau) u''(\tau) d\tau + r_n \int_{\tau_{n-2}}^{\tau_{n-1}} (\tau - \tau_{n-2}) u''(\tau) d\tau \right|$$

$$\leq C \left(k_n^2 \tau_{n-1}^{-3/2} + k_n k_{n-1} \tau_{n-2}^{-3/2} \right). \tag{4.51}$$

Furthermore, from (4.46) we immediately obtain

$$|d^n| \leq C \left(k_n^2 \tau_{n-1}^{-5/2} + k_n k_{n-1} \tau_{n-2}^{-5/2} \right) + C \left(k_n^2 \tau_{n-1}^{-3/2} + k_n k_{n-1} \tau_{n-2}^{-3/2} \right), \tag{4.52}$$

which implies the desired consistency estimate (4.49) for the scheme (4.2).

For the IMEX Euler scheme, $n \geq 2$, it follows from (4.47) that $|\tilde{d}_2^n| \leq C k_n \tau_{n-1}^{-1/2}$. Using this estimate and conditions (3.10) and (4.6), we obtain the desired consistency estimate (4.50) for the IMEX Euler scheme. ∎

4.4. Error estimates. In this subsection, we derive the error bound for the variable step-size IMEX BDF2 method for PIDE (4.2).

THEOREM 4.4. *Let $\mathfrak{B} \subset V$ be a bounded set, let $T < 1$, and let $r_{\max} \leq R$ with $1 < R < \bar{R} \approx 1.91$. Take $k_1 < \frac{\mu}{2\gamma_1^2}$. If $u(\tau) \in \mathfrak{B}$ for $0 \leq \tau \leq T$, then for sufficiently small step-sizes $0 < k_n \leq k_{\max}$, the error $e^n = u(\tau_n) - u^n$ $(n = 2, 3, \ldots, N)$ satisfies*

$$|e^n| \leq C \left(k_1^{1/2} + k_2^{1/2} + \sum_{j=3}^{n} k_j^2 \left(k_j \tau_{j-1}^{-5/2} + k_{j-1} \tau_{j-2}^{-5/2} \right) \right). \tag{4.53}$$

Proof. It follows from (3.2) and (4.2) that

$$\bar{\partial}_B^2 e^n + \mathcal{A} e^n + \mathcal{B}_1 e^n + \mathcal{B}_2 E e^{n-1} + \mathcal{J}(E e^{n-1}) = d^n, \quad n \geq 2. \tag{4.54}$$

Then we may apply Theorem 4.2 to obtain, with C independent of N,

$$|e^n| \leq C \left(|e^0| + k_1 (\|e^1\| + \|e^0\|) + \sum_{j=1}^{n} k_j |d^j| \right). \tag{4.55}$$

Now that $e^0 = 0$, we need to estimate the initial step error e^1 produced by the IMEX Euler method (4.4). It follows from (3.2) and (4.4) that

$$\bar{\partial}_B^1 e^1 + \mathcal{A} e^1 + \mathcal{B}_1 e^1 + \mathcal{B}_2 e^0 + \mathcal{J}(e^0) = d^1. \tag{4.56}$$

Take in (4.56) the inner product with $k_1 e^1$ to obtain

$$\frac{1}{2} \left(|e^1|^2 - |e^0|^2 + |e^1 - e^0|^2 \right) + \mu k_1 \|e^1\|^2$$
$$\leq \gamma_1 k_1 \|e^1\| |e^1| + \gamma_2 k_1 \|e^0\| |e^1| + C_J k_1 |e^0| |e^0| + k_1 |d^1| |e^1|,$$

and therefore, in view of $e^0 = 0$,

$$|e^1|^2 + \mu k_1 \|e^1\|^2 \leq \frac{\mu k_1}{2} \|e^1\|^2 + \frac{\gamma_1^2}{2\mu} k_1 |e^1|^2 + k_1^2 |d^1|^2 + \frac{1}{4} |e^1|^2. \tag{4.57}$$

Using the condition

$$\frac{\gamma_1^2}{2\mu}k_1 \le c_4 < \frac{1}{4},$$

we further get

$$|e^1|^2 + \mu k_1 \|e^1\|^2 \le k_1^2 |d^1|^2. \tag{4.58}$$

From (4.48), by Theorem 3.1, we have

$$|d^1| \le \frac{1}{k_1}\int_0^{\tau_1} \tau |u''(\tau)| d\tau + C\int_0^{\tau_1} |u'(\tau)| d\tau \le C k_1^{-1/2}. \tag{4.59}$$

Substitute (4.59) into (4.58) to obtain

$$|e^1|^2 + \mu k_1 \|e^1\|^2 \le C k_1. \tag{4.60}$$

For d^2, we have

$$\begin{aligned} |d^2| &\le \frac{C}{k_2}\int_{\tau_1}^{\tau_2} (\tau_1 - \tau)^2 |u'''(\tau)| d\tau + \frac{C}{k_2}\int_0^{\tau_2} \tau^2 |u'''(\tau)| d\tau \\ &\quad + \int_{\tau_1}^{\tau_2} |(\tau_2 - \tau) u''(\tau)| d\tau + r_2 \int_0^{\tau_1} |\tau u''(\tau)| d\tau \\ &\le C k_2 k_1^{-3/2} + \frac{C\tau_2^{1/2}}{k_2} + C k_2 k_1^{-1/2} + C k_1^{1/2}. \end{aligned} \tag{4.61}$$

With (4.56) and (4.59)–(4.61), we obtain

$$|e^n| \le C\left(k_1 + \sum_{j=1}^{n} k_j |d^j|\right) \tag{4.62}$$

and therefore the desired result. This completes the proof. ∎

We end this section with some remarks.

The first remark is about T. In Theorem 4.4, we assume $T < 1$. This is because singularities may arise at $\tau = 0$, and the time regularity result in Theorem 3.1 is valid for $T < 1$. For $T \ge 1$, we can split $[0, T]$ into $[0, T_1]$ and $[T_1, T]$ with $T_1 < 1$. Then the result in Theorem 4.4 can be applied to the IMEX BDF2 method for a PIDE on the interval $[0, T_1]$. As for the numerical solution on $[T_1, T]$, since the solution to PIDE (3.2) generally has higher regularity on $[T_1, T]$, it is easy to show that the variable step-size IMEX BDF2 method is second-order accurate.

The second remark is about the step-sizes k_1 and k_2. The error estimate (4.53) suggests that to obtain uniform accuracy, k_j, $j = 1, 2, 3, 4$, should take smaller values than k_j, $j > 4$.

5. Two possible choices for time grids. Theorem 4.4 reveals that due to the nonsmoothness of the initial data $g(x)$, it is beneficial to take smaller time steps near $\tau = 0$. There are two possible choices for time grids in the literature to accomplish this.

5.1. Choice 1 for time grid: $J^{N,1}$. This is accomplished by choosing the approximation times τ_n according to [46],

$$\tau_n = \begin{cases} \left(\frac{1-\varpi_1^{n/(2N-4)}}{1-\varpi_1}\right) T, & n = 0,1,2,3, \\ \left(\frac{1-\varpi_1^{(n-2)/(N-2)}}{1-\varpi_1}\right) T, & n = 4,5,\ldots,N, \end{cases} \tag{5.1}$$

where ϖ_1 is a constant greater than one. Observe that the time steps near the expiry $t = T$, i.e., $\tau = 0$, become smaller by increasing ϖ_1.

Let $\psi_N := \varpi_1^{\frac{1}{2N-4}}$. Then it is easy to obtain $k_1 = \frac{1-\psi_N}{1-\varpi_1}$, $k_n = \psi_N^{n-1} k_1$, $n = 2,3,4$, and $k_n = \psi_N^{2(n-3)}(1+\psi_N)k_1$, $n = 5,6,\ldots,N$. We get $r_n = \psi_N$, $n = 2,3,4$, $r_5 = \psi_N(1+\psi_N)$, and $r_n = \psi_N^2$, $n = 6,\ldots,N$. Consequently, we have $\Phi_N = r_5 - r_7 = \psi_N$.

5.2. Choice 2 for time grid: $J^{N,2}$. Let us choose the time levels τ_n according to $\tau_n = T(n/N)^{\varpi_2}$ with $\varpi_2 \geq 1$. Note that $\varpi_2 = 1$ corresponds to constant step-size (see [5]). In [5] it was observed that Φ_N is bounded since r_n is decreasing. Following the approach of Becker [5], we may apply Theorem 4.4 to obtain, for $0 \leq n \leq N$,

$$\begin{aligned} |e^n| &\leq C\left(N^{-\varpi_2/2} + N^{-2}\sum_{j=1}^{N-1}\frac{1}{N}\left(\frac{j}{N}\right)^{-3+\varpi_2/2}\right) \\ &\leq \begin{cases} CN^{-\varpi_2/2}, & \varpi_2 < 4, \\ CN^{-2}\log N, & \varpi_2 = 4, \\ CN^{-2}, & \varpi_2 > 4. \end{cases} \end{aligned} \tag{5.2}$$

6. Fully discrete approximation of option pricing problems. The aim of this section is to discretize the parabolic equation (2.6) in space using the finite difference method on $\Omega = (X_l, X_r)$. It is noteworthy that since the time discretization is independent of the choice of spatial discretization, for spatial discretization one can use other techniques also, e.g., finite element, spectral method, etc.

6.1. Finite difference discretization of spatial derivatives. Here we describe the discretization of the spatial derivative terms, together with the zeroth-order term, that is, the operator

$$\mathcal{L}u(\tau,x) = -\frac{1}{2}\sigma^2\frac{\partial^2 u}{\partial x^2} - \left(r_I - \frac{1}{2}\sigma^2 - \lambda\kappa\right)\frac{\partial u}{\partial x} + (r_I+\lambda)u. \tag{6.1}$$

We have truncated the infinite domain $\mathbb{R}$ for x to be $\bar{\Omega} = [X_l, X_r]$. A uniform mesh $X_l = x_0 < \cdots < x_{i-1} < x_i < x_{i+1} < \cdots < x_M = X_r$ will be used. The space derivatives of (6.1) are approximated with central finite differences

$$\frac{\partial u}{\partial x}(\tau,x_i) \approx \frac{u_{i+1}(\tau) - u_{i-1}(\tau)}{2h}, \quad \frac{\partial^2 u}{\partial x^2}(\tau,x_i) \approx \frac{u_{i+1}(\tau) - 2u_i(\tau) + u_{i-1}(\tau)}{h^2}, \tag{6.2}$$

where $h = x_{i+1} - x_i$, and $u_i(\tau)$ denotes the approximation of $u(\tau,x_i)$. Then it follows that

$$\begin{aligned} \mathcal{L}_h u_i(\tau) = &-\frac{1}{2}\sigma^2\left[\frac{u_{i+1}(\tau) - 2u_i(\tau) + u_{i-1}(\tau)}{h^2}\right] \\ &-\left(r_I - \frac{1}{2}\sigma^2 - \lambda\kappa\right)\frac{u_{i+1}(\tau) - u_{i-1}(\tau)}{2h} + (r_I+\lambda)u_i(\tau), \end{aligned} \tag{6.3}$$

which will lead to a tridiagonal matrix denoted by D, which has off-diagonal elements

$$D_{i,i-1} = \frac{-\sigma^2 + (r_I - \frac{1}{2}\sigma^2 - \lambda\kappa)h}{2h^2}, \qquad D_{i,i+1} = \frac{-\sigma^2 - (r_I - \frac{1}{2}\sigma^2 - \lambda\kappa)h}{2h^2}.$$

It is well known that the finite difference discretization $\mathcal{L}_h u$ is a second-order accurate approximation to $\mathcal{L}u$. Also, for sufficiently small h, we know that the off-diagonal elements of D will be nonpositive, and thus D will be an M-matrix.

6.2. Approximating integrals. In this subsection we consider the discretization of the integral operator

$$\mathcal{I}u(\tau, x) = \int_\Omega u(\tau, x + y) f(y) dy. \tag{6.4}$$

By making the change of variable $y = z - x$, we obtain

$$\int_\Omega u(\tau, x + y) f(y) dy = \int_{x+X_l}^{x+X_r} u(\tau, z) f(z - x) dz.$$

Let $f_{i,j} := f(x_j - x_i)$. Using the composite trapezoidal rule on the interval $\Omega^* = (x + X_l, x + X_r)$, we obtain the following approximation of the integral:

$$\int_{\Omega^*} u(\tau, z) f(z - x_i) dz \approx \frac{h}{2}\left[f_{i,0} u_0 + f_{i,M} u_M + 2 \sum_{j=1}^{M-1} f_{i,j} u_j \right]. \tag{6.5}$$

The discrete matrix will be denoted by P. It is easy to show that our approximation of the integral is second-order accurate.

6.3. Stability and convergence of fully discrete scheme. The stability and convergence analysis carried out in section 4 can be extended to the fully discrete case. Following the approach of [50] or standard technique for the finite difference method, we can obtain the same stability result in the norm

$$|v| := \left(\sum_{i=1}^{M-1} h v_i^2 \right)^{1/2}, \tag{6.6}$$

which mimics the L^2 norm, for the fully discrete approximation under a similar time step restriction of $\tilde{C}_\epsilon k_{\max} \le 1$ with $\tilde{C}_\epsilon$ independent of h.

To estimate the fully discrete error $e_i^n = u(\tau_n, x_i) - u_i^n$, where u_i^n are the fully discrete approximations of $u(\tau_n, x_i)$, we use the relation $e_i^n = e^n + \hat{e}_i^n = u(\tau_n, x_i) - u^n(x_i) + u^n(x_i) - u_i^n$. The time discrete error e^n has been estimated in Theorem 4.4. Since the discrete approximations for differential and integral operators are second-order accurate, using the stability result for the fully discrete approximation, we have

$$|\hat{e}^n| \le Ch^2,$$

and therefore the final estimate,

$$|e^n| \le C \left(k_1^{1/2} + k_2^{1/2} + \sum_{j=3}^{n} k_j^2 \left(k_j \tau_{j-1}^{-5/2} + k_{j-1} \tau_{j-2}^{-5/2} \right) + h^2 \right), \tag{6.7}$$

where C is independent of k_n and h.

6.4. Local mesh refinement. Since the financial payoff function is given by (2.5), the nonsmooth region is around the strike price $S = K$. Therefore, it is necessary to concentrate grid points near $x^* = 0$.

Assume that the spatial direction is first discretized by a uniform mesh with initial mesh size $h_0 = h = \frac{X_r - X_l}{M}$, where $M + 1$ is the beginning number of grid points in the x-direction. Choosing x^* and four points closest to x^*, that is

$$x^* - 2h_0, \quad x^* - h_0, \quad x^*, \quad x^* + h_0, \quad x^* + 2h_0,$$

inserting the first points ($L_0 = 4$) among them, and letting $h_1 = h_0/2$, we obtain

$$x^* - 2h_0,\ \underline{x^* - 3h_1},\ x^* - h_0,\ \underline{x^* - h_1},\ x^*,\ \underline{x^* + h_1},\ x^* + h_0,\ \underline{x^* + 3h_1},\ x^* + 2h_0.$$

Choosing x^* and four points among them, and letting $L_0 = 8, h_2 = h_1/2$, we obtain

$$x^* - h_0,\ \underline{\underline{x^* - 3h_2}},\ \underline{x^* - h_1},\ \underline{\underline{x^* - h_2}},\ x^*,\ \underline{\underline{x^* + h_2}},\ \underline{x^* + h_1},\ \underline{\underline{x^* + 3h_2}},\ x^* + h_0.$$

Repeat the above steps until some h_i reaches the stopping criterion $h_i \le h_0^2$; see, e.g., [31, 10].

7. Numerical experiments. Using several numerical examples, we now illustrate the theoretical results of the previous sections. We price European options under Merton's and Kou's jump-diffusion models. For simplicity, we consider the case when μ_{Me}, σ_{Me}, σ, and λ are constants since in this case the price of a European option can be expressed as an infinite sum [36] for Merton's model,

$$U(t, S) = \sum_{n=0}^{\infty} \frac{(\lambda'\tau)^n}{n!} e^{-\lambda'\tau} V_{BS}(S, \tau, K, \zeta_n, \sigma_n), \tag{7.1}$$

where $\tau = T - t$, $\tau \in [0, T]$, $S \in [S_{\min}, S_{\max}]$, and

$$\lambda' = \lambda(1 + \kappa), \quad \sigma_n^2 = \sigma^2 + \frac{n\sigma_{\text{Me}}^2}{\tau}, \quad \zeta_n = r_I - \lambda\kappa + \frac{n}{\tau}\left(\mu_{\text{Me}} + \frac{1}{2}\sigma_{\text{Me}}^2\right).$$

$V_{BS}(S, \tau, K, \zeta_n, \sigma_n)$ is the Black–Scholes formula for the option value when there are no jumps, that is

$$V_{BS}(S, \tau, K, \zeta_n, \sigma_n) = \begin{cases} S\mathcal{N}(d_1) - Ke^{-\zeta_n\tau}\mathcal{N}(d_2) & \text{in the case of a call option,} \\ Ke^{-\zeta_n\tau}\mathcal{N}(-d_2) - S\mathcal{N}(-d_1) & \text{in the case of a put option,} \end{cases}$$

where

$$d_1 = \frac{\ln(\frac{S}{K}) + (\zeta_n + \frac{\sigma_n^2}{2})\tau}{\sigma_n\sqrt{\tau}}, \qquad d_2 = \frac{\ln(\frac{S}{K}) + (\zeta_n - \frac{\sigma_n^2}{2})\tau}{\sigma_n\sqrt{\tau}} = d_1 - \sigma_n\sqrt{\tau}.$$

The formula (7.1) is easily implemented, and normally only the first five or six terms in the sum are needed to obtain six digits of accuracy in the option price.

Example 1 (European call option under Merton's model). In our first numerical example, we price a European call option and illustrate the convergence orders of the IMEX BDF2 methods with different choices for time grids.

Let the parameters in the model be (see, e.g., [14, 29, 25])

$$\sigma = 0.15, \quad r_I = 0.05, \quad \mu_{\text{Me}} = -0.9, \quad \sigma_{\text{Me}} = 0.45,$$
$$\lambda = 0.1, \quad T = 0.25, \quad K = 100, \quad X_l = -1.5, \quad X_r = 1.5.$$

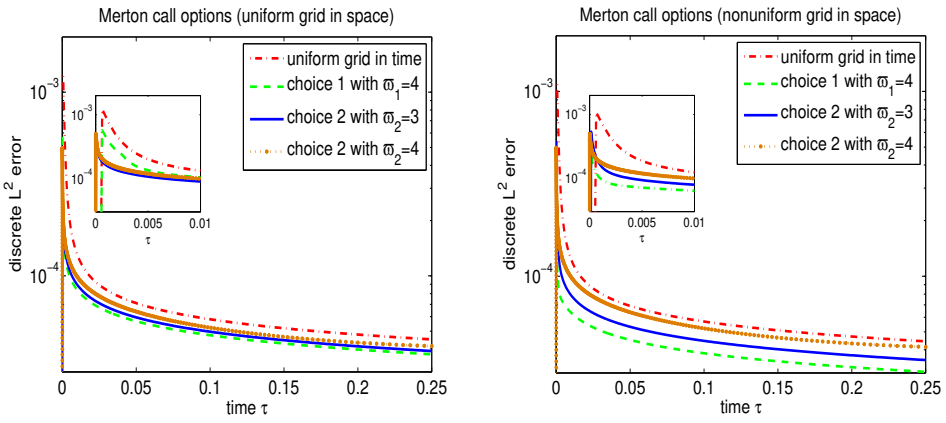

FIG. 1. *The time evolution of the discrete L^2 error* (6.6) *of Merton's call option produced by the variable step-size IMEX BDF*2 *scheme with four different time grids, where* $M = 2048$ *and* $N = 400$. *Left: uniform grid in space. Right: nonuniform grid in space.*

The reference values obtained by using (7.1) for European call option under Merton's model are 0.52763802 at $S = 90$, 4.39124569 at $S = 100$, and 12.64340583 at $S = 110$.

In this example, the spatial differential operator $\mathcal{L}$ is implicitly treated by using finite difference methods, and the jump integral is explicitly computed using the composite trapezoidal rule; that is, the operator $\mathcal{L}$ in (6.1) is split into $\mathcal{A} + \mathcal{B}_1 + \mathcal{B}_2$ with $\mathcal{B}_2 \equiv 0$. Let the convergence order be calculated by using the double grid principle

$$\text{Order} = \log_2(E_i^{N,M}/E_i^{2N,2M}) \quad \text{or} \quad \text{Order} = \log_2(E_i^{N,M}/E_i^{2N,M}),$$

where $E_i^{N,M}$ denotes the error computed at the maturity date T and $x = x_i$ with N time subintervals and M spatial subintervals. We choose M and N as done in [14, 29, 25].

We present the pricing errors and the convergence orders of the variable step-size IMEX BDF2 scheme with different choices for time grids (choice 1 (5.1) with $\varpi_1 = 4$, choice 2 with $\varpi_2 = 3$, and choice 2 with $\varpi_2 = 4$) in Tables 1–3, respectively. From these numerical results, we observe that the variable step-size IMEX BDF2 scheme is of order two for all three time grids when the space mesh is uniform. As for the nonuniform space mesh, although irregular refinement of local mesh refinement may affect the convergence order of the scheme, the errors produced by the scheme with local mesh refinement are smaller than those without local mesh refinement. We also note that the errors of the variable step-size IMEX BDF2 scheme on $J^{N,1}$ (choice 1) with $\varpi_1 = 4$ are smaller than those of the scheme on $J^{N,2}$ with $\varpi_2 = 4$. These are demonstrated in Figure 1. To clearly illustrate that the proposed variable step-size IMEX BDF2 method is more accurate, we also present the discrete L^2 errors near $\tau = 0$ on a large scale.

Example 2 (European put option under Merton's model). In this numerical example, we price a European put option and show the errors of the IMEX BDF2 methods with different choices for time grids. As earlier, spatial differential operator $\mathcal{L}$ is implicitly treated, and the jump integral is explicitly computed using the composite trapezoidal rule.

TABLE 1

The value of European call option under Merton's model obtained by the variable step-size IMEX BDF2 scheme with choice 1 ($\varpi_1 = 4$) and the convergence orders of the scheme. Top rows: without local mesh refinement. Bottom rows: with local mesh refinement.

		S=90		S=100		S=110	
M	N	Error	Order	Error	Order	Error	Order
128	25	4.4805E-03		3.5462E-02		8.1249E-03	
256	50	6.8515E-04	2.7092	8.7658E-03	2.0163	2.0789E-03	1.9666
512	100	1.5734E-04	2.1225	2.1866E-03	2.0032	5.2204E-04	1.9936
1024	200	3.9700E-05	1.9867	5.4648E-04	2.0004	1.3059E-04	1.9992
2048	400	1.0055E-05	1.9812	1.3663E-04	1.9999	3.2643E-05	2.0002
		$S = 90$		$S = 100$		$S = 110$	
M	N	Error	Order	Error	Order	Error	Order
128	25	8.7342E-04		1.6931E-02		2.4493E-03	
256	50	3.1907E-04	1.4528	6.9773E-03	1.2789	1.0647E-03	1.2020
512	100	8.5934E-05	1.8926	2.0215E-03	1.7873	3.7427E-04	1.5082
1024	200	2.1868E-05	1.9744	5.2992E-04	1.9316	1.1080E-04	1.7561
2048	400	5.4912E-06	1.9936	1.3482E-04	1.9748	3.0088E-05	1.8806

TABLE 2

The value of European call option under Merton's model obtained by the variable step-size IMEX BDF2 scheme with choice 2 ($\varpi_2 = 3$) and the convergence orders of the scheme. Top rows: without local mesh refinement. Bottom rows: with local mesh refinement.

		S=90		S=100		S=110	
M	N	Error	Order	Error	Order	Error	Order
128	25	3.6462E-03		3.4031E-02		8.5092E-03	
256	50	1.0294E-03	1.8245	8.4176E-03	2.0154	2.1686E-03	1.9723
512	100	2.6405E-04	1.9630	2.0995E-03	2.0033	5.4366E-04	1.9960
1024	200	6.6434E-05	1.9908	5.2466E-04	2.0006	1.3591E-04	2.0001
2048	400	1.6637E-05	1.9976	1.3116E-04	2.0000	3.3965E-05	2.0005
		S=90		S=100		S=110	
M	N	Error	Order	Error	Order	Error	Order
128	25	3.1144E-03		1.8190E-02		2.4963E-03	
256	50	3.6383E-04	3.0976	7.2787E-03	1.3214	1.0860E-03	1.2007
512	100	7.9513E-05	2.1940	2.0944E-03	1.7971	3.8064E-04	1.5126
1024	200	2.0547E-05	1.9523	5.4785E-04	1.9347	1.1250E-04	1.7584
2048	400	5.3038E-06	1.9538	1.2927E-04	1.9759	3.0528E-05	1.8818

TABLE 3

The value of European call option under Merton's model obtained by the variable step-size IMEX BDF2 scheme with choice 2 ($\varpi_2 = 4$) and the convergence orders of the scheme. Top rows: without local mesh refinement. Bottom rows: with local mesh refinement.

		S=90		S=100		S=110	
M	N	Error	Order	Error	Order	Error	Order
128	25	5.1389E-03		3.2409E-02		8.9850E-03	
256	50	1.4436E-03	1.8318	8.0415E-03	2.0108	2.2752E-03	1.9815
512	100	3.6989E-04	1.9644	2.0074E-03	2.0022	5.6855E-04	2.0007
1024	200	9.3108E-05	1.9901	5.0177E-04	2.0002	1.4193E-04	2.0021
2048	400	2.3329E-05	1.9968	1.2545E-04	1.9999	3.5448E-05	2.0014
		S=90		S=100		S=110	
M	N	Error	Order	Error	Order	Error	Order
128	25	7.3904E-03		1.4204E-02		3.2789E-03	
256	50	1.4856E-03	2.3146	6.2635E-03	1.1813	1.2582E-03	1.3818
512	100	3.6340E-04	2.0314	1.8425E-03	1.7653	4.2069E-04	1.5806
1024	200	9.1785E-05	1.9852	4.8521E-04	1.9250	1.2214E-04	1.7842
2048	400	2.3141E-05	1.9878	1.2364E-04	1.9724	3.2893E-05	1.8927

Let the parameters in the model be (see, e.g., [24])

$$\sigma = 0.3, \quad r_I = 0, \quad \mu_{\mathrm{Me}} = 0, \quad \sigma_{\mathrm{Me}} = 0.5,$$
$$\lambda = 1.0, \quad T = 0.5, \quad K = 100, \quad X_l = -2, \quad X_r = 2.$$

The reference values for European put option under Merton's model are 20.41168240 at $S = 90$, 15.03495881 at $S = 100$, and 10.95077346 at $S = 110$.

To clearly illustrate the convergence order of the variable step-size IMEX BDF2 method, in this example we consider different numbers N of time grid points, together with the same space grid, $M = 2048$. The numerical results are listed in Table 4.

TABLE 4

The value of European put option under Merton's model obtained by the variable step-size IMEX BDF2 scheme with uniform grid in space and three choices in time. Top rows: choice 1 ($\varpi_1 = 4$). Middle rows: choice 2 ($\varpi_2 = 3$). Bottom rows: choice 2 ($\varpi_2 = 4$).

		S=90		S=100		S=110	
M	N	Error	Order	Error	Order	Error	Order
2048	25	1.0172E-02		1.3546E-02		8.7341E-03	
2048	50	2.5957E-03	1.9704	3.3877E-03	1.9995	2.2371E-03	1.9650
2048	100	6.3981E-04	2.0204	8.1897E-04	2.0484	5.3817E-04	2.0555
2048	200	1.4367E-04	2.1549	1.7344E-04	2.2394	1.0460E-04	2.3632
2048	400	1.8774E-05	2.9359	1.1663E-05	3.8945	4.8665E-06	4.4258
2048	25	1.6329E-02		2.2019E-02		1.3938E-02	
2048	50	4.2536E-03	1.9407	5.5888E-03	1.9781	3.6675E-03	1.9262
2048	100	1.0684E-03	1.9933	1.3793E-03	2.0186	9.1147E-04	2.0085
2048	200	2.5251E-04	2.0810	3.1477E-04	2.1316	1.9985E-04	2.1893
2048	400	4.6196E-05	2.4505	4.7148E-05	2.7390	1.9184E-05	3.3810
2048	25	4.0056E-03		5.4032E-03		3.3331E-03	
2048	50	9.2847E-04	2.1091	1.2262E-03	2.1397	7.6385E-04	2.1255
2048	100	2.0813E-04	2.1574	2.6395E-04	2.2158	1.5502E-04	2.3009
2048	200	3.3946E-05	2.6162	3.2928E-05	3.0029	2.9492E-05	2.3940
2048	400	8.8783E-06	1.9349	1.3681E-05	1.2671	6.9943E-06	2.0761

The time evolution of the discrete L^2 errors of the numerical results on $[0, 0.5]$ is shown in Figure 2. The local enlarged drawings of the discrete L^2 errors on the time interval $[0, 0.01]$ are also presented in Figure 2. As analyzed in section 5, from Table 4 and Figure 2, we observe that the variable step-size IMEX BDF2 scheme on $J^{N,2}$ (choice 2) with $\varpi_2 = 4$ has higher accuracy and higher convergence order than the variable step-size IMEX BDF2 scheme on $J^{N,2}$ with $\varpi_2 = 3$ when the space grid is uniform. From Figure 2, we also see that the errors of the variable step-size IMEX BDF2 scheme on $J^{N,1}$ (choice 1) with $\varpi_2 = 4$ are generally larger than those of the scheme on $J^{N,2}$ with $\varpi_2 = 4$. A comparison with the results of Example 1 reveals that the two variable grids considered in section 5 have their own advantages. From the theoretical results presented in Theorem 4.4 and Figures 1–2, we observe the following important fact: compared with the constant step-size IMEX BDF2 method, the variable step-size IMEX BDF2 method is superior, since it has much smaller errors (especially near $\tau = 0$) than the constant step-size IMEX BDF2 method.

Example 3 (European put option under Kou's model). Let the parameters in the model be (see, e.g., [14, 29, 40, 24])

$$\sigma = 0.15, \quad r_I = 0.05, \quad a = 0.3445, \quad \eta_1 = 3.0465, \quad \eta_2 = 3.0775,$$
$$\lambda = 0.1, \quad T = 0.25, \quad K = 100, \quad X_l = -1.5, \quad X_r = 1.5.$$

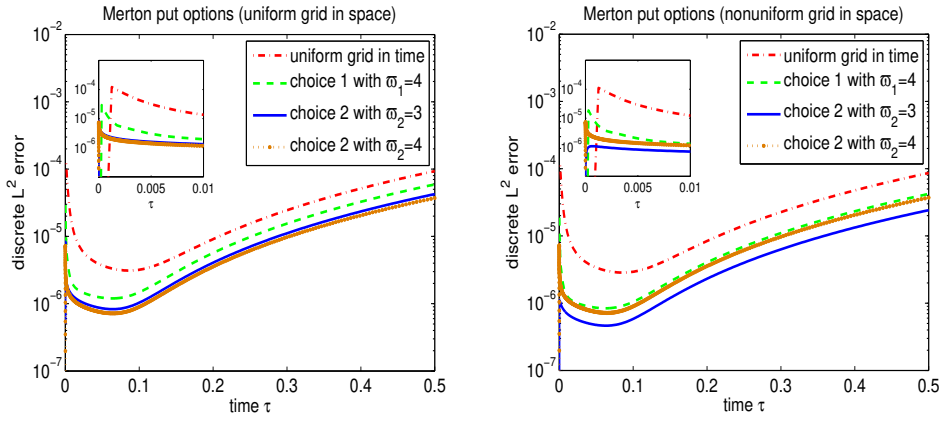

FIG. 2. *The time evolution of the discrete L^2 error* (6.6) *of Merton's put option obtained by the variable step-size IMEX BDF*2 *scheme with four different time grids, where* $M = 2048$ *and* $N = 400$. *Left: uniform grid in space. Right: nonuniform grid in space.*

The reference values for the European put option under Kou's model are 9.430457 at $S = 90$, 2.731259 at $S = 100$, and 0.552363 at $S = 110$ [29].

The purpose of this numerical experiment is to illustrate the effect of explicitly treating the lower-order derivative term on the convergence order of the variable step-size IMEX BDF2 method. For this purpose, we consider two different splittings for operator $\mathcal{L}$ in (6.1): one is $\mathcal{L} = \mathcal{A}+\mathcal{B}_1+\mathcal{B}_2$ with $\mathcal{B}_2 = -\left(r - \frac{1}{2}\sigma^2 - \lambda\kappa\right)\frac{\partial}{\partial x}$; the other is $\mathcal{L} = \mathcal{A}+\mathcal{B}_1+\mathcal{B}_2$ with $\mathcal{B}_2 = (r+\lambda)I$, where I is the identical operator. As considered in section 4, we will treat operator $\mathcal{B}_2$ explicitly. The numerical results of the variable step-size IMEX BDF2 method with the convection term $\mathcal{B}_2 = -\left(r - \frac{1}{2}\sigma^2 - \lambda\kappa\right)\frac{\partial}{\partial x}$ being explicitly treated are listed in Table 5. The numerical results of explicitly treating the reaction term $\mathcal{B}_2 = (r+\lambda)I$ are reported in Table 6. For these different IMEX combinations, we still observe the correct order of convergence for the variable step-size IMEX BDF2 method from Tables 5 and 6. This further confirms our theoretical analysis.

8. Concluding remarks. In this work we considered the stability and error estimates of the variable step-size IMEX BDF2 method applied to the abstract PIDE (3.2) with nonsmooth initial data, which describes the jump-diffusion option pricing model in finance. We first obtained time regularity results of the solution to PIDE (3.2) when the initial data was $u^0 \in V$. Due to the nonsmoothness of the initial data, singularities may arise at $\tau = 0$. Hence it is beneficial to take smaller time steps near $\tau = 0$ and use the variable step-size IMEX BDF2 method for solving this type of equation. In the literature, much work has been done on IMEX schemes for pricing options, since in this way we avoid having to solve the dense algebraical system. To the best of our knowledge, however, this is the first paper where the variable step-size IMEX BDF2 method is employed to solve PIDEs with nonsmooth initial data in an option pricing context. We showed that the variable step-size IMEX BDF2 method is stable for abstract PIDEs under a suitable time step restriction which depends on the choice of the operator $\mathcal{B}_2$ explicitly treated. Based on the time regularity analysis of abstract PIDEs, we derived the consistency error and the global error bounds for

TABLE 5

The value of European put option under Kou's model obtained by the variable step-size IMEX BDF2 method on uniform mesh in space with the convection term being explicitly treated. Top rows: uniform mesh in time. Middle rows: choice 1 ($\varpi_1 = 4$). Bottom rows: choice 2 ($\varpi_2 = 4$).

		S=90		S=100		S=110	
M	N	Error	Order	Error	Order	Error	Order
128	25	2.0606E-02		2.5170E-02		2.4569E-02	
256	50	5.1116E-03	2.0112	6.2588E-03	2.0078	6.1171E-03	2.0059
512	100	1.2532E-03	2.0281	1.5425E-03	2.0206	1.5094E-03	2.0189
1024	200	2.9009E-04	2.1110	3.6415E-04	2.0827	3.5757E-04	2.0777
2048	400	4.9467E-05	2.5520	6.9607E-05	2.3872	6.9579E-05	2.3615
128	25	1.2946E-02		1.2829E-02		1.0234E-02	
256	50	3.1895E-03	2.0212	3.2824E-03	1.9666	2.6790E-03	1.9336
512	100	7.7235E-04	2.0460	8.1025E-04	2.0183	6.6611E-04	2.0079
1024	200	1.6986E-04	2.1849	1.8247E-04	2.1507	1.4865E-04	2.1638
2048	400	1.9409E-05	3.1296	2.4354E-05	2.9055	1.7583E-05	3.0797
128	25	1.0097E-02		3.4608E-03		1.1385E-02	
256	50	2.2210E-03	2.1847	9.2707E-04	1.9004	2.8643E-03	1.9909
512	100	4.9982E-04	2.1517	2.5943E-04	1.8373	7.3532E-04	1.9617
1024	200	9.8028E-05	2.3501	8.7109E-05	1.5745	2.0354E-04	1.8530
2048	400	9.9433E-07	6.6233	4.3311E-05	1.0081	6.0689E-05	1.7458

TABLE 6

The value of European put option under Kou's model obtained by the variable step-size IMEX BDF2 method on uniform mesh in space with the reaction term being explicitly treated. Top rows: uniform mesh in time. Middle rows: choice 1 ($\varpi_1 = 4$). Bottom rows: choice 2 ($\varpi_2 = 4$).

		S=90		S=100		S=110	
M	N	Error	Order	Error	Order	Error	Order
128	25	1.4657E-02		1.8913E-02		1.7932E-02	
256	50	3.6380E-03	2.0104	4.6993E-03	2.0089	4.4585E-03	2.0079
512	100	8.8631E-04	2.0373	1.1532E-03	2.0268	1.0947E-03	2.0260
1024	200	1.9854E-04	2.1584	2.6689E-04	2.1113	2.5388E-04	2.1084
2048	400	2.6601E-05	2.8999	4.5298E-05	2.5587	4.3654E-05	2.5399
128	25	1.3938E-02		1.8079E-02		1.8405E-02	
256	50	3.4509E-03	2.0140	4.4960E-03	2.0076	4.5550E-03	2.0146
512	100	8.3875E-04	2.0407	1.1026E-03	2.0277	1.1163E-03	2.0287
1024	200	1.8656E-04	2.1686	2.5426E-04	2.1166	2.5898E-04	2.1079
2048	400	2.3594E-05	2.9832	4.2143E-05	2.5930	4.4892E-05	2.5283
128	25	1.4275E-02		1.7409E-02		2.0937E-02	
256	50	3.5278E-03	2.0167	4.3752E-03	1.9924	5.2198E-03	2.0040
512	100	8.5713E-04	2.0412	1.0771E-03	2.0222	1.2865E-03	2.0205
1024	200	1.9104E-04	2.1657	2.4839E-04	2.1165	3.0201E-04	2.0908
2048	400	2.4698E-05	2.9514	4.0733E-05	2.6084	5.5707E-05	2.4386

the variable step-size IMEX BDF2 method. Since the variable step-size IMEX BDF2 method allows us to take different time step-sizes for different time scales, i.e., small time step-sizes for the time domain with solution rapidly varying, and large step-sizes for the time domain with solution slowly changing, it demonstrates the prominent advantages of high accuracy compared to the constant step-size IMEX BDF2 method.

We have implemented various numerical experiments for the variable step-size IMEX BDF2 method for European options under Merton's and Kou's models. For both models, these experiments exactly verify the theoretical results. The second-order accuracy is maintained for two types of time variable grid. These numerical experiments suggest that the variable step-size IMEX BDF2 method is more accurate than the popular constant step-size IMEX BDF2 method. Thus, the variable step-size IMEX BDF2 method is especially efficient for pricing options.

We have also implemented a numerical experiment for the variable step-size IMEX BDF2 method for the American put option under Merton's model. The parameters, which have been considered in [13, 30], are the same as those in the example of the European call option under Merton's model (Example 1). We notice that the American option satisfies a linear complementarity problem (LCP) (see, e.g., [13, 28]),

$$\begin{cases} \frac{\partial u}{\partial \tau} + \mathcal{L}u - \lambda \mathcal{I}u - \lambda R(\tau, x) \geq 0, \qquad u - g \geq 0, \\ \Big(\frac{\partial u}{\partial \tau} + \mathcal{L}u - \lambda \mathcal{I}u - \lambda R(\tau, x)\Big)(u - g) = 0, \end{cases} \tag{8.1}$$

with the same initial value as in (2.7). The boundary conditions for the American put option are given by [13, 30]

$$u(\tau, X_l) = K - Ke^{X_l} \quad \text{and} \quad u(\tau, X_r) = 0.$$

We use the penalty method proposed by d'Halluin, Forsyth, and Labahn in [13] (see also [47, 9]) with penalty parameter $\varepsilon = 10^{-4}$ to solve the LCP. The reference values for the American put option under Merton's model are 10.003822 at $S = 90$, 3.241251 at $S = 100$, and 1.419803 at $S = 110$ (see, e.g., [30]). The numerical results are listed in Table 7. From Table 7, we observe that the order of convergence for all quantities is 2, though our theoretical results do not hold for the American option (PID inequality) due to the nonsmoothness of the solution near the free boundary or inequality constraints. With realistic regularity assumptions on the data and a mild step-size restriction, Kadalbajoo, Tripathi, and Kumar showed in [26] that a finite element method (FEM) combined with two IMEX time discretizations (viz. IMEX Euler and BDF2) converges with rate $\mathcal{O}(\sqrt{k} + h)$ in the single-asset case and rate $\mathcal{O}(\sqrt{k} + \sqrt{h})$ in the multi-asset (two and three assets) case in another norm. Compared with these interesting results, our numerical results can be viewed as a prospect for future work.

TABLE 7

The value of American put option under Merton's model obtained by the variable step-size IMEX BDF2 scheme and the convergence orders of the scheme. Top rows: choice 1 *($\varpi_1 = 4$). Bottom rows: choice* 2 *($\varpi_2 = 4$).*

		S=90		S=100		S=110	
M	N	Error	Order	Error	Order	Error	Order
50	20	8.4585E-02		1.1258E-01		1.1030E-01	
100	40	2.1051E-02	2.0065	2.7846E-02	2.0155	2.7305E-02	2.0141
200	80	5.2431E-03	2.0054	6.9333E-03	2.0058	6.7988E-03	2.0058
400	160	1.2887E-03	2.0245	1.7127E-03	2.0173	1.6799E-03	2.0169
800	320	2.9930E-04	2.1062	4.0696E-04	2.0733	4.0024E-04	2.0694
1600	640	5.1812E-05	2.5303	8.0342E-05	2.3406	8.0254E-05	2.3182
50	20	6.6383E-02		8.5532E-02		9.4696E-02	
100	40	1.5950E-02	2.0573	2.1022E-02	2.0246	2.2861E-02	2.0504
200	80	3.9101E-03	2.0283	5.1950E-03	2.0167	5.6281E-03	2.0221
400	160	9.4853E-04	2.0434	1.2732E-03	2.0287	1.3800E-03	2.0280
800	320	2.1342E-04	2.1520	2.9641E-04	2.1028	3.2436E-04	2.0890
1600	640	3.0236E-05	2.8193	5.2620E-05	2.4939	6.1173E-05	2.4066

Acknowledgments. The authors would like to thank the two referees for comments and suggestions that led to improvements in the presentation of this paper.

REFERENCES

[1] Y. Achdou and O. Pironneau, *Computational Methods for Option Pricing*, Frontiers Appl. Math., 30, SIAM, Philadelphia, 2005, https://doi.org/10.1137/1.9780898717495.

[2] A. Almendral and C. W. Oosterlee, *Numerical valuation of options with jumps in the underlying*, Appl. Numer. Math., 53 (2005), pp. 1–18, https://doi.org/10.1016/j.apnum.2004.08.037.

[3] L. Andersen and J. Andreasen, *Jump-diffusion processes: Volatility smile fitting and numerical methods for option pricing*, Rev. Derivatives Res., 4 (2000), pp. 231–262, https://doi.org/10.1023/A:1011354913068.

[4] G. Barles and H. M. Soner, *Option pricing with transaction costs and a nonlinear Black-Scholes equation*, Finance Stoch., 2 (1998), pp. 369–397, https://doi.org/10.1007/s007800050046.

[5] J. Becker, *A second order backward difference method with variable steps for a parabolic problem*, BIT, 38 (1998), pp. 644–662, https://doi.org/10.1007/BF02510406.

[6] F. Black and M. Scholes, *The pricing of options and corporate liabilities*, J. Polit. Econ., 81 (1973), pp. 637–654, https://doi.org/10.1086/260062.

[7] M. Briani, R. Natalini, and G. Russo, *Implicit–explicit numerical schemes for jump–diffusion processes*, Calcolo, 44 (2007), pp. 33–57, https://doi.org/10.1007/s10092-007-0128-x.

[8] P. Carr, H. Geman, D. B. Madan, and M. Yor, *The fine structure of asset returns: An empirical investigation*, J. Bus., 75 (2002), pp. 305–332, https://doi.org/10.1086/338705.

[9] Y. Chen, W. Wang, and A. Xiao, *An efficient algorithm for options under Merton's jump-diffusion model on nonuniform grids*, 53 (2019), 1565–1591, https://doi.org/10.1007/s10614-018-9823-8.

[10] Y. Chen, A. G. Xiao, and W. S. Wang, *An IMEX-BDF2 compact scheme for pricing options under regime-switching jump-diffusion models*, Math. Methods Appl. Sci., 42 (2019), pp. 2646–2663.

[11] R. Cont and P. Tankov, *Financial Modelling with Jump Processes*, Chapman & Hall/CRC, Boca Raton, FL, 2004.

[12] R. Cont and E. Voltchkova, *A finite difference scheme for option pricing in jump diffusion and exponential Lévy models*, SIAM J. Numer. Anal., 43 (2005), pp. 1596–1626, https://doi.org/10.1137/S0036142903436186.

[13] Y. d'Halluin, P. A. Forsyth, and G. Labahn, *A penalty method for American options with jump diffusion processes*, Numer. Math., 97 (2004), pp. 321–352, https://doi.org/10.1007/s00211-003-0511-8.

[14] Y. d'Halluin, P. A. Forsyth, and K. R. Vetzal, *Robust numerical methods for contingent claims under jump diffusion processes*, IMA J. Numer. Anal., 25 (2005), pp. 87–112, https://doi.org/10.1093/imanum/drh011.

[15] C. M. Elliott and S. Larsson, *Error estimates with smooth and nonsmooth data for a finite element method for the Cahn-Hilliard equation*, Math. Comp., 58 (1992), pp. 603–630, https://doi.org/10.1090/S0025-5718-1992-1122067-1.

[16] E. Emmrich, *Stability and error of the variable two-step BDF for semilinear parabolic problems*, J. Appl. Math. Comput., 19 (2005), pp. 33–55, https://doi.org/10.1007/BF02935787.

[17] L. Feng and V. Linetsky, *Pricing options in jump-diffusion models: An extrapolation approach*, Oper. Res., 56 (2008), pp. 304–325, https://doi.org/10.1287/opre.1070.0419.

[18] R. Frey and P. Patie, *Risk Management for Derivatives in Illiquid Markets: A Simulation Study*, in Advances in Finance and Stochastics, K. Sandmann and P. Schönbucher, eds., Springer, Berlin, 2002, pp. 137–159, https://doi.org/10.1007/978-3-662-04790-3_8.

[19] B. Gaviraghi, M. Annunziato, and A. Borzía, *Analysis of splitting methods for solving a partial integro-differential Fokker–Planck equation*, Appl. Math. Comput., 294 (2017), pp. 1–17, https://doi.org/10.1016/j.amc.2016.08.050.

[20] J. Guo and W. Wang, *An unconditionally stable, positivity-preserving splitting scheme for nonlinear Black-Scholes equation with transaction costs*, Sci. World J., (2014), 525207, https://doi.org/10.1155/2014/525207.

[21] J. Guo and W. Wang, *On the numerical solution of nonlinear option pricing equation in illiquid markets*, Comput. Math. Appl., 69 (2015), pp. 117–133, https://doi.org/10.1016/j.camwa.2014.11.015.

[22] D. Henry, *Geometric Theory of Semilinear Parabolic Equations*, Lecture Notes in Math. 840, Springer-Verlag, Berlin, 1981, https://doi.org/10.1007/BFb0089647.
[23] M. K. Kadalbajoo, L. P. Tripathi, and A. Kumar, *Second order accurate IMEX methods for option pricing under Merton and Kou jump-diffusion model*, J. Sci. Comput., 65 (2015), pp. 979–1024, https://doi.org/10.1007/s10915-015-0001-z.
[24] M. K. Kadalbajoo, A. Kumar, and L. P. Tripathi, *An efficient numerical method for pricing option under jump diffusion model*, Int. J. Adv. Eng. Sci. Appl. Math., 7 (2015), pp. 114–123, https://doi.org/10.1007/s12572-015-0136-z.
[25] M. K. Kadalbajoo, A. Kumar, and L. P. Tripathi, *A radial basis function based implicit–explicit method for option pricing under jump-diffusion models*, Appl. Numer. Math., 110 (2016), pp. 159–173, https://doi.org/10.1016/j.apnum.2016.08.006.
[26] M. K. Kadalbajoo, L. P. Tripathi, and A. Kumar, *An error analysis of a finite element method with IMEX-time semidiscretizations for some partial integro-differential inequalities arising in the pricing of American options*, SIAM J. Numer. Anal., 55 (2017), pp. 869–891, https://doi.org/10.1137/16M1074746.
[27] S. G. Kou, *A jump diffusion model for option pricing*, Management Sci., 48 (2002), pp. 1086–1101, https://doi.org/10.1287/mnsc.48.8.1086.166.
[28] A. Kunoth, Chr. Schneider, and K. Wiechers, *Multiscale methods for the valuation of American options with stochastic volatility*, Int. J. Comput. Math., 89 (2012), pp. 1145–1163, https://doi.org/10.1080/00207160.2012.672732.
[29] Y. Kwon and Y. Lee, *A second-order finite difference method for option pricing under jump-diffusion models*, SIAM J. Numer. Anal., 49 (2011), pp. 2598–2617, https://doi.org/10.1137/090777529.
[30] Y. Kwon and Y. Lee, *A second-order tridiagonal method for American options under jump-diffusion models*, SIAM J. Sci. Comput., 33 (2011), pp. 1860–1872, https://doi.org/10.1137/100806552.
[31] S. T. Lee and H.-W. Sun, *Fourth-order compact scheme with local mesh refinement for option pricing in jump-diffusion model*, Numer. Methods Partial Differential Equations, 28 (2012), pp. 1079–1098, https://doi.org/10.1002/num.20677.
[32] H. E. Leland, *Option pricing and replication with transaction costs*, J. Finance, 40 (1985), pp. 1283–1301, https://doi.org/10.2307/2328113.
[33] T. J. Lyons, *Uncertain volatility and the risk-free synthesis of derivatives*, Appl. Math. Finance, 2 (1995), pp. 117–133, https://doi.org/10.1080/13504869500000007.
[34] A.-M. Matache, C. Schwab, and T. P. Wihler, *Fast numerical solution of parabolic integrodifferential equations with applications in finance*, SIAM J. Sci. Comput., 27 (2007), pp. 365–393, https://doi.org/10.1137/030602617.
[35] R. C. Merton, *Theory of rational option pricing*, Bell J. Econom. Management Sci., 4 (1973), pp. 141–183, https://doi.org/10.2307/3003143.
[36] R. C. Merton, *Option pricing when underlying stock returns are discontinuous*, J. Financ. Econom., 3 (1976), pp. 125–144, https://doi.org/10.1016/0304-405X(76)90022-2.
[37] E. Pindza, K. C. Patidar, and E. Ngounda, *Robust spectral method for numerical valuation of European options under Merton's jump-diffusion model*, Numer. Methods Partial Differential Equations, 30 (2014), pp. 1169–1188, https://doi.org/10.1002/num.21864.
[38] J. A. Rad and K. Parand, *Pricing American options under jump-diffusion models using local weak form meshless techniques*, Int. J. Comput. Math., 94 (2017), pp. 1694–1718, https://doi.org/10.1080/00207160.2016.1227434.
[39] J. A. Rad and K. Parand, *Numerical pricing of American options under two stochastic factor models with jumps using a meshless local Petrov–Galerkin method*, Appl. Numer. Math., 115 (2017), pp. 252–274, https://doi.org/10.1016/j.apnum.2017.01.015.
[40] S. Salmi and J. Toivanen, *An iterative method for pricing American options under jump–diffusion models*, Appl. Numer. Math., 61 (2011), pp. 821–831, https://doi.org/10.1016/j.apnum.2011.02.002.
[41] S. Salmi and J. Toivanen, *IMEX schemes for pricing options under jump–diffusion models*, Appl. Numer. Math., 84 (2014), pp. 33–45, https://doi.org/10.1016/j.apnum.2014.05.007.
[42] S. Salmi, J. Toivanen, and L. von Sydow, *An IMEX-scheme for pricing options under stochastic volatility models with jumps*, SIAM J. Sci. Comput., 36 (2014), pp. B817–B834, https://doi.org/10.1137/130924905.
[43] D. Schötzau and C. Schwab, *Time discretization of parabolic problems by the hp-version of the discontinuous Galerkin finite element method*, SIAM J. Numer. Anal., 38 (2000), pp. 837–875, https://doi.org/10.1137/S0036142999352394.
[44] L. von Sydow, J. Toivanen, and C. Zhang, *Adaptive finite differences and IMEX time-stepping to price options under Bates model*, Int. J. Comput. Math., 92 (2015), pp. 2515–2529, https://doi.org/10.1080/00207160.2015.1072173.

[45] D. Tavella and C. Randall, *Pricing Financial Instruments: The Finite Difference Method*, John Wiley & Sons, Chichester, UK, 2000.
[46] J. Toivanen, *Numerical valuation of European and American options under Kou's jump-diffusion model*, SIAM J. Sci. Comput., 30 (2008), pp. 1949–1970, https://doi.org/10.1137/060674697.
[47] W. S. Wang and Y. Chen, *Fast numerical valuation of options with jump under Merton's model*, J. Comput. Appl. Math., 318 (2017), pp. 79–92, https://doi.org/10.1016/j.cam.2016.11.038.
[48] K. Yosida, *Functional Analysis*, Springer-Verlag, New York, 1965, https://doi.org/10.1007/978-3-662-25762-3.
[49] K. Zhang and S. Wang, *A computational scheme for options under jump-diffusion processes*, Int. J. Numer. Anal. Model., 6 (2009), pp. 110–123.
[50] X. L. Zhang, *Numerical analysis of American option pricing in a jump-diffusion model*, Math. Oper. Res., 22 (1997), pp. 668–690, https://doi.org/10.1287/moor.22.3.668.